Dipole Solvation in Nondipolar Solvents: Experimental Studies of Reorganization Energies and Solvation Dynamics†

ARTICLE *in* THE JOURNAL OF PHYSICAL CHEMISTRY · JUNE 1996

Impact Factor: 2.78 · DOI: 10.1021/jp953110e

Dipole Solvation in Nondipolar Solvents: Experimental Studies of Reorganization Energies and Solvation Dynamics†

L. Reynolds, J. A. Gardecki, S. J. V. Frankland, M. L. Horng, and M. Maroncelli*

Department of Chemistry, 152 Davey Laboratory, The Pennsylvania State University, University Park, Pennsylvania 16802

Received: October 20, 1995; In Final Form: December 20, 1995⊗

Steady-state and time-resolved emission measurements of the solvatochromic probe coumarin 153 are used to study solvation of a dipolar solute in nondipolar solvents such as benzene and 1,4-dioxane. Contrary to the predictions of dielectric continuum theories, the Stokes shifts (or nuclear reorganization energies) that accompany electronic excitation of this solute are substantial in such solvents (∼1000 cm^{-1}). The magnitudes of the shifts observed in both nondipolar and dipolar solvents can be consistently understood in terms of the relative strength of the interactions between the permanent charge distributions of the solute and solvent molecules. (Information concerning these charge distributions is derived from extensive *ab initio* calculations on the solute and 31 common solvents.) The dynamics of solvation in nondipolar solvents, as reflected in the time dependence of the Stokes shifts, is qualitatively like that observed in polar solvents. But, whereas the dynamics in polar solvents can be rather simply modeled using the solvents dielectric response as empirical input, no simple theories of this sort are currently capable of predicting the solvation dynamics in nondipolar solvents.

I. Introduction

Understanding the solvation of polar solutes in polar solvents has been the goal of a great many studies for nearly half a century. Much of what is known about the energetics involved comes from electronic spectroscopy, where frequency shifts between gas and solution phase, or among different solvents (solvatochromism), serve to probe differences between the solvation of two electronic states. Since the earliest theories on the nature of such solvent-induced shifts,[1] it has been known that reasonable estimates of solvation energies can be obtained from simple cavity-dipole/dielectric continuum treatments. Such treatments have often been criticized for their neglect of molecular aspects of solvation, as well as for their reliance on imprecisely defined cavity constructs. Nevertheless, numerous studies have shown that when specific solute−solvent interactions are absent, these theories provide an excellent starting point for understanding the energetics of real solute/solvent systems.[2] Over the past decade attention has shifted from the equilibrium energetics of solvation to time-dependent aspects of solvation in polar solvents.[3−5] Perhaps surprisingly, continuum dielectric models have again proven to have considerable predictive value in modeling the dynamics in such systems.

One of the best demonstrations of the success of continuum dielectric theories for modeling both the static and dynamic aspects of polar solvation was provided by recent studies of the probe solute coumarin 153 (C153, below).[5] As will be discussed in more detail later, electronic excitation of C153 leads to a charge redistribution that is predominantly dipolar in character. The dipole moment of C153 increases by approximately 8 D between the S_0 and S_1 states, and this change leads to a time-dependent shift of the emission spectrum of more than 2000 cm^{-1} in strongly polar solvents such as acetonitrile. Measurement of this time-dependent shift provides useful information about both the energetics and the dynamics of the solvation process. The magnitude of the "dynamic Stokes shift" reflects the nuclear reorganization energy in a given solvent, and the time dependence of the emission frequency provides the solvation response function pertaining to the dipolar solute perturbation. For a wide range of dipolar solvents, including even alcohols and other hydrogen-bonding solvents, it was found that both the reorganization energies and the time dependence of the solvation response could be reasonably modeled by dielectric continuum descriptions of solvation.

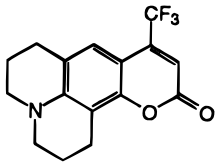

Coumarin 153

However, this same study also pointed out examples where such descriptions are clearly inadequate. These cases involved solvents that might naively be called nonpolar, the prime example being benzene. C153 undergoes a time-dependent emission shift in benzene that is qualitatively similar to the shifts observed in highly polar solvents. While the magnitude of the shift is only about half as large as in a solvent like acetonitrile, it is still quite substantial and easily measured. Continuum dielectric models, which work well for describing many polar solvents, completely fail to account for the shifts in benzene and related molecules. Such models predict *no* shift of the emission spectrum of C153 in benzene, due to the fact that benzene has no dipole moment. Continuum models, because they rely solely on the infinite wavelength dielectric properties of the solvent (ϵ_0 or $\epsilon(\omega)$), do not distinguish between truly *nonpolar* solvents, cyclohexane for example, and *nondipolar* solvents like benzene. By nonpolar we mean solvents that lack any strongly polar bonds. Benzene and related molecules are not nonpolar in this sense. They may, for symmetry reasons, have a net zero dipole moment, but they still contain significantly polar bonds which can lead to large higher-order multipole moments (quadrupole, octapole, etc.). Although such higher moments or local bond polarities cannot produce a

† Presented at the Northeast Regional ACS Meeting in Rochester, NY (October 24 and 25, 1995), on the "Structure and Dynamics of Liquids".

⊗ Abstract published in *Advance ACS Abstracts,* May 15, 1996.

S0022-3654(95)03110-8 CCC: $12.00

macroscopic polarization and thus be detected in infinite wavelength dielectric experiments, they may still be quite effective in solvating a molecular solute like C153. Dielectric continuum models are completely unable to treat these nondipolar but nevertheless "polar" solvents.

In the present study, we continue our previous work on C153 in order to focus specifically on understanding the nature of solvation in benzene and other nondipolar solvents. To this end we have expanded the earlier measurements of the steady-state solvatochromism of C153[5] to include many more nondipolar solvents. Using steady-state data and the "time-zero" method,[6] we have estimated the magnitudes of the dynamic Stokes shift (or nuclear reorganization energies) associated with the dipole solvation of C153 in a wide range of both dipolar and nondipolar solvents. These results are presented in section III, where we also make comparisons to two commonly used solvatochromic scales of solvent polarity. Such comparisons indicate that the Stokes shifts of C153 provide a new and distinct measure of the "nuclear polarizability" (as distinguished from the electronic polarizability) of solvents which is not available from other polarity scales. In section IV we describe extensive *ab initio* electronic structure calculations of many of the solvent molecules examined in experiment. We show that a first-pass understanding of the magnitude of the reorganization energies observed in nondipolar solvents can be obtained from a knowledge of the quadrupole moments of the solvent molecules. In section V we examine the energetics of probe−solvent interactions more closely, through electrostatic modeling of pairwise interactions between C153 and the various solvent molecules. We show that the reorganization energies observed in both dipolar and nondipolar solvents can be consistently explained solely on the basis of interactions between the permanent charge distribution of solvent molecules and the difference charge distribution (S_1-S_0) of the solute. Finally, in section VI we consider the time dependence of the solvation response measured for several of the nondipolar solvents. We show that the dynamics in nondipolar and weakly dipolar solvents are quite similar, and both appear to be simply related to the single-particle dynamics of solvent molecules.

II. Experimental Procedures

Coumarin 153 was purchased from Exciton Inc. (laser grade) and was used as received. Solvents were obtained from Aldrich and were of HPLC grade whenever available. With few exceptions these solvents were also used as received.

Steady-state absorption and emission measurements were performed using Perkin-Elmer Lambda 6 and Spex Fluorolog F212 spectrometers, respectively. Instrumental parameters were chosen to provide resolutions of 1 nm in absorption and ∼2 nm in emission. Fluorescence spectra were corrected for the wavelength response of the instrument. Both absorption and emission spectra were converted to a linear frequency representation prior to analysis. Most samples for the steady-state measurements were contained in 1 cm quartz cuvettes and were made up to optical densities of ∼1 and ∼0.1 in absorption and emission, respectively. These optical densities correspond to solute concentrations of roughly 5×10^{-4} and 5×10^{-5} M. All measurements on liquid solvents were performed at room temperature, 22 ± 2 °C. For measurements in the supercritical solvents CO_2 and CHF_3, a stainless steel high-pressure cell with a 1.5 cm sample path length was used. The temperatures (∼35 °C) and pressures (∼1500 psi) employed in these measurements were chosen such that the density of the solvent was comparable to those of typical liquid solvents. (See Table 1.)

Time-resolved emission data were obtained using a fluorescence up-conversion spectrometer that is described in detail in ref 5. The system uses the doubled output of a 70 fs Ti:sapphire laser for sample excitation (∼385 nm) and reflective optics for collection and refocusing of the emission. The overall instrumental response is ∼120 fs (fwhm). Time-resolved spectra were reconstructed from a series of 10−12 decays spanning the steady-state emission spectrum. A detailed description of the methods of data fitting and spectral reconstruction can be also found in ref 5.

III. Steady-State Spectroscopy and Dipole Reorganization Energies

Many aspects of the solvatochromic behavior of C153 have been described at length in ref 5. We will therefore only mention those points most important to the present work and refer the reader to this previous source for more details. As will be discussed in section V, the solvatochromism of C153 results primarily from the large increase (about 8 D) in dipole moment between its ground (S_0) and first excited singlet (S_1) states. Typical examples of the sorts of solvent-dependent spectra observed with this probe are shown in Figure 1, where we have plotted the steady-state absorption and emission spectra (solid curves) of C153 in the solvents 2-methylbutane (2MB), benzene, and acetonitrile. Two characteristic changes are observed as one progresses from 2MB to benzene to acetonitrile. The spectra broaden, as signaled by the loss of vibronic structure present in the 2MB spectra, and also shift to the red by several thousand wavenumbers. (Note that the benzene and acetonitrile spectra have been plotted such that the absorption shift is not apparent in Figure 1.) These frequency and width changes are direct (and interrelated[7]) consequences of the increasing strength of solute−solvent interactions in this series of solvents.

While the individual shifts of the absorption and emission spectra (and/or their widths) all contain information about the energetics of solvation, we will focus on a slightly more complicated observable, the magnitude of the dynamic Stokes shift, $\Delta\nu = \nu(0) - \nu(\infty)$. $\Delta\nu$ is the time-dependent shift that the emission spectrum undergoes subsequent to excitation at $t = 0$. It measures the change in the solvation energies of the S_0 and S_1 electronic states due only to repolarization of the nuclear degrees of freedom of the solvent, i.e., the energetics exclusive of the solvent electronic response. This nuclear component of solvation is of interest because it is the equivalent of the solvent reorganization energy relevant in the coupling between a solvent and a system undergoing electron transfer.[8] In section VI we will discuss actual time-dependent emission measurements. However, we have previously shown that the magnitude of the dynamic Stokes shift can be derived with good accuracy using data from steady-state spectra alone.[5,6]

The method for determining $\Delta\nu$ from steady-state spectra, as well as the approximations involved, are described in detail in refs 5 and 6. Briefly, the analysis entails comparing both absorption and emission spectra in a "polar" solvent of interest to spectra recorded in a reference solvent for which the nuclear repolarization is expected to be negligible. We use the 2-methylbutane as the reference solvent here. From comparisons of the absorption spectra one deduces the inhomogeneous line-broadening function (assumed Gaussian) that best reproduces the observed polar spectrum from the reference 2MB spectrum. (The dotted curves in Figure 1 illustrate the quality of the fits typically obtained in this way.) The same line-broadening function is then applied to the emission line shape in 2MB in order to provide the estimate for the "time-zero"

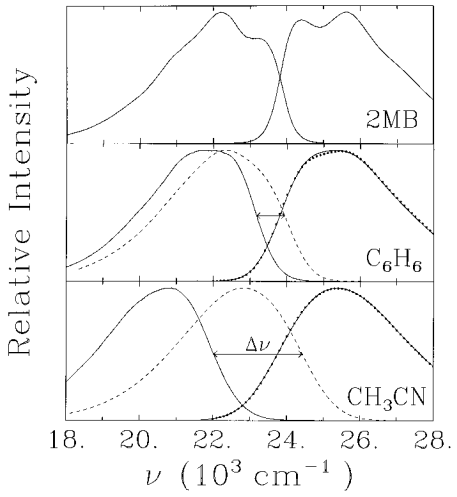

Figure 1. Steady-state spectra of C153 in 2-methylbutane ("2MB"), benzene ("C_6H_6"), and acetonitrile ("CH_3CN"). The solid curves in each figure are the absorption and steady-state emission spectra observed in the respective solvents. The dotted curves superimposed in the benzene and acetonitrile absorption spectra are the fits to these spectra described in the text. The dashed curves in the lower panels are estimated "time-zero" spectra, the spectra expected prior to any solvent relaxation. The method for generating these time-zero spectra is discussed in the text and described in more detail in refs 5 and 6. As illustrated here, the difference between the latter spectra and the steady-state emission spectra provides the measure of the magnitude of the time-dependent Stokes shift ($\Delta\nu$) we employ here. Note that the frequencies of the spectra in benzene and acetonitrile have been shifted by 1241 and 1739 cm^{-1}, respectively, so that the origins of the absorption and time-zero spectra coincide in all solvents.

spectrum, the emission spectrum that would be observed in the polar solvent prior to any solvent nuclear motion. Such time-zero estimates for C153 in benzene and acetonitrile are shown as the dashed curves in Figure 1. The value of $\Delta\nu$ obtained from the difference between this estimated time-zero spectrum and the steady-state emission spectrum is comparable to what one calculates from simply referring the difference between the absorption and emission maxima in the solvent of interest to this same difference in 2MB, as is sometimes done in solvatochromic studies. However, the present method provides more accurate estimates of the reorganization energy. We note that, for the collection of 24 solvents whose dynamics were time resolved in ref 5, an average absolute deviation of only 90 cm^{-1} was found between the observed dynamic Stokes shifts and the values of $\Delta\nu$ determined using the time-zero method. We will therefore apply this method in the present studies in order to determine the nuclear reorganization energies of C153 in a wide range of solvents.

A summary of the spectral characteristics of C153 in 48 common solvents is provided in Table 1. While our primary interest is in the magnitudes of the dynamic Stokes shifts, we have, for the sake of completeness, also included in Table 1 a listing of other features (first-moment frequency and full width) of the individual absorption and emission spectra as well as parameters defining the time-zero spectra. In Table 1 and the following tables we have divided solvents into three categories. The first category consists of what we will call "simple dipolar" solvents. This group (no. 1−25) includes all nonassociating solvents with dipole moments greater than 1 D, together with several hydrocarbon solvents having negligible dipole moments. The second class of solvents we will refer to as "nondipolar". These solvents (no. 31−44) are ones that, by virtue of exact or near symmetry, have dipole moments that are exactly or approximately zero, but which nevertheless contain bonds that are expected to be significantly polar. Included in this class are solvents like benzene, 1,4-dioxane, and carbon dioxide. The final category of solvents includes all those (no. 51−59) which can act as hydrogen-bond donors. We have previously shown that such hydrogen-bonding ability plays little or no role in the shifts observed with C153.[6] We keep them separated here only to make comparison to empirical polarity scales easier.

In ref 5 we showed that the magnitude of the Stokes shift of C153 in many solvents can be well understood in terms of dielectric theories of solvation. The simplest of such theories treats the solute as an Onsager-type cavity dipole and the solvent as a structureless fluid. This type of theory predicts that the solvent dependence of $\Delta\nu$ should be confined to a reaction field factor of the form

$$F(\epsilon_0,n) = \frac{\epsilon_0 - 1}{\epsilon_0 + 2} - \frac{n^2 - 1}{n^2 + 2} \qquad (1)$$

where ϵ_0 is the static dielectric constant and n the refractive index of the solvent. Figure 2 shows a plot of the Stokes shifts observed with C153 as a function of this reaction field factor. There is a reasonable correlation between $\Delta\nu$ and $F(\epsilon_0,n)$ in both the dipolar and the hydrogen-bonding solvents. Simple continuum theories would predict that $\Delta\nu$ should be proportional to $F(\epsilon_0,n)$ and that the proportionality constant is related to the change in dipole moment ($\Delta\mu$) between the S_0 and S_1 states of the solute. The line drawn in Figure 2 shows the proportionality fit to the data from the 34 solvents in categories i and iii (correlation coefficient $R = 0.94$). It has a slope of 3000 ± 150 (95%), which, with an appropriate choice of cavity radius,[5] is of the magnitude expected for $\Delta\mu \sim 8$ D. Thus, although there is considerable scatter in the data, both simple dipolar and hydrogen-bonding solvents can be adequately modeled in terms of continuum dielectric descriptions of solvation. However, Figure 2 also shows that there are many solvents, those in the nondipolar category, for which such dielectric modeling fails. Solvents comprised of molecules without appreciable permanent dipole moments cannot generate long-range polarization of the sort that is measured in dielectric (ϵ_0) experiments. Thus, all solvents in this category are predicted by continuum theories to have nuclear polarization responses, as measured by $F(\epsilon_0,n)$, that are essentially zero. The fact that the observed Stokes shifts in many such solvents lie in the range 500−1000 cm^{-1} is a clear indication that this kind of dielectric modeling is inappropriate for predicting reorganization energies in these cases. But, apart from this departure from continuum expectations, there is nothing qualitatively different about the spectra of C153 in these nondipolar solvents. For example, apart from an origin shift (δ_0 in Table 1), the absorption and emission spectra of C153 in benzene ($F \sim 0$) are virtually indistinguishable from the spectra in the dipolar solvent diethyl ether ($F \sim 0.3$), for which $F(\epsilon_0,n)$ *does* serve as an appropriate polarity indicator.

What is the source of the "anomalous" shifts observed in nondipolar solvents? For solvents with significantly polar bonds, even in the absence of a net dipole moment, rotation and translation of those solvent molecules nearest to the solute should serve to modulate its solvation energy. A clear illustration of this point is provided by comparing the two solvents 1,4-dioxane and tetrahydrofuran (THF). One expects the local bond polarities of the CH_2-O-CH_2 groups in dioxane and THF to be similar. The main difference between these two solvents is that, whereas the presence of a single such group in tetrahydrofuran leads to an appreciable dipole moment (1.75 D), the two groups in dioxane oppose one another in such a

TABLE 1: Summary of Solvent Properties and Steady-State Spectral Data

		solvent properties[b]						characteristics of steady-state and "time-zero" spectra[c]						Stokes shift[d]
solvent	no.	μ	ϵ_0	n_D	$F(\epsilon_0,n)$	π^*	E_N^T	$\bar{\nu}_{abs}$	Γ_{abs}	$\bar{\nu}_{em}$	Γ_{em}	δ_0	Γ_{inh}	$\Delta\nu$
acetonitrile	1	3.53	35.9	1.342	0.71	0.66	0.460	24.38	3.89	18.35	3.27	1.74	1.70	2.32 (10)
propylene carbonate	2	4.94	64.9	1.420	0.70	0.83	0.472	24.05	3.90	18.26	3.27	1.99	1.71	2.11 (10)
propionaldehyde	3	2.54	18.5	1.359	0.63	0.71		24.31	3.87	18.48	3.36	1.69	1.67	2.08 (10)
dimethyl sulfoxide	4	4.06	46.5	1.478	0.66	1.00	0.444	23.74	3.91	18.03	3.32	2.21	1.71	2.02 (12)
dimethylformamide	5	3.24	36.7	1.428	0.67	0.88	0.386	23.95	3.89	18.24	3.26	2.03	1.67	1.98 (13)
nitromethane	6	3.56	35.9	1.380	0.69	0.75	0.481	24.10	3.83	18.37	3.18	1.99	1.61	1.92 (10)
acetone	7	2.69	20.6	1.356	0.65	0.62	0.355	24.41	3.87	18.69	3.30	1.65	1.64	1.84 (11)
methyl acetate	8	1.72	6.7	1.359	0.43	0.49	0.253	24.73	3.83	19.18	3.37	1.32	1.50	1.65 (10)
HMPA	9	4.31	29.3	1.457	0.63	0.87	0.315	23.82	3.84	18.41	3.28	2.25	1.54	1.63 (10)
cyclohexanone	10	3.08	16.1	1.450	0.57	0.68	0.281	24.22	3.79	18.78	3.29	1.76	1.49	1.60 (12)
fluoroform ($\rho = 0.84$)	11	1.65	6.2	1.145	0.54			25.55	3.82	19.87	3.37	0.66	1.47	1.55 (20)
ethyl acetate	12	1.82	6.0	1.370	0.40	0.45	0.228	24.75	3.81	19.36	3.47	1.27	1.43	1.43 (10)
tetrahydrofuran	13	1.75	7.6	1.405	0.44	0.55	0.207	24.69	3.79	19.35	3.36	1.39	1.40	1.31 (12)
benzonitrile	14	4.01	25.2	1.526	0.58	0.88	0.333	23.96	3.68	18.75	3.16	2.06	1.24	1.28 (14)
dichloromethane	15	1.14	8.9	1.421	0.47	0.73	0.309	24.21	3.68	19.15	3.20	1.77	1.21	1.11 (13)
1,2-difluorobenzene	16	2.40	14.3	1.443	0.55	0.72	0.265	24.40	3.71	19.40	3.28	1.59	1.25	1.10 (10)
diethylamine	17	1.19	3.9	1.383	0.26	0.35	0.145	25.01	3.73	19.89	3.43	1.02	1.16	1.04 (10)
1,3-difluorobenzene	18	1.58	5.2	1.437	0.32	0.50	0.204	24.72	3.71	19.89	3.31	1.26	1.12	0.86 (10)
1-chlorobutane	19	1.90	7.4	1.400	0.44	0.40		24.57	3.69	19.91	3.35	1.22	1.13	0.85 (10)
chloroform	20	1.15	4.8	1.443	0.29	0.69	0.259	24.37	3.83	19.52	3.20	1.67	1.07	0.79 (12)
diethyl ether	21	1.15	4.2	1.350	0.30	0.24	0.117	25.18	3.72	20.32	3.47	0.84	1.06	0.75 (10)
diisopropyl ether	22	1.38	3.9	1.366	0.27	0.19	0.105	25.26	3.69	20.60	3.41	0.75	0.92	0.55 (10)
1,1,2-TCTF ethane	23	<.4	2.4	1.356	0.10	0.01	0.077	25.61	3.66	21.02	3.46	0.44	0.78	0.36 (10)
2-methylbutane	24	0.00	1.8	1.351	0.00	−0.15	0.006	26.13	3.66	21.74	3.38	0.00	0.00	0.00 (10)
cyclohexane	25	0.00	2.0	1.424	−0.00	0.00	0.006	25.98	3.57	21.75	3.48	0.09	0.00	−0.04 (10)
1,4-dioxane	31	0.45	2.2	1.420	0.03	0.49	0.164	24.96	3.82	19.74	3.35	1.02	1.36	1.24 (10)
1,2,4,5-TFbenzene	32			1.407	0.00			24.90	3.73	20.01	3.34	1.07	1.15	0.92 (10)
1,4-difluorobenzene	33	0.00	2.3	1.441	0.03	0.49	0.176	24.80	3.72	20.00	3.31	1.18	1.10	0.82 (10)
1,4-xylene	34	0.02	2.3	1.493	0.01	0.45	0.074	24.87	3.67	20.07	3.48	1.09	0.99	0.74 (10)
benzene	35	0.00	2.3	1.498	0.01	0.55	0.111	24.77	3.65	20.00	3.31	1.24	1.00	0.72 (10)
hexafluorobenzene	36	0.33	2.1	1.375	0.03	0.27	0.108	25.20	3.71	20.46	3.36	0.83	1.07	0.65 (10)
carbon dioxide ($\rho = 0.80$)	37	0.00	∼1.4	1.193	0.00	−0.06	0.030	26.29	4.13	21.24	3.65	−.06	1.18	0.65 (10)
toluene	38	0.31	2.4	1.494	0.02	0.49	0.099	24.82	3.67	20.20	3.35	1.14	0.97	0.59 (10)
n-butylbenzene	39	0.36	2.4	1.487	0.02			24.92	3.66	20.28	3.41	1.03	0.88	0.58 (10)
1,3,5-trifluorobenzene	40	∼0	∼2	1.414	0.00	0.18	0.077	25.40	3.72	20.90	3.32	0.54	0.84	0.44 (10)
carbon tetrachloride	41	0.00	2.3	1.460	0.03	0.21	0.052	25.77	3.89	21.61	3.39	0.67	0.65	0.30 (20)
carbon disulfide	42	0.06	2.6	1.627	0.00	0.51	0.065	24.75	3.30	20.43	3.17	1.37	0.52	0.09 (10)
perfluorohexane	43	∼0	1.6	1.252	0.00	−0.48		26.45	3.54	22.18	3.54	−.51	0.19	0.08 (13)
methanol	51	1.7	32.7	1.327	0.71	0.60	0.762	24.02	3.97	17.99	3.07	2.04	1.85	2.47 (10)
ethanol	52	1.66	24.6	1.359	0.67	0.54	0.654	24.08	3.88	18.10	3.18	1.95	1.72	2.23 (17)
1-propanol	53	1.7	20.5	1.384	0.63	0.52	0.617	24.13	3.84	18.30	3.17	1.92	1.53	2.00 (18)
2-propanol	54	1.66	19.9	1.375	0.63	0.48	0.546	24.16	3.81	18.41	3.37	1.89	1.56	1.95 (10)
1-butanol	55	1.75	17.5	1.397	0.61	0.47	0.586	24.12	3.84	18.32	3.18	1.90	1.63	2.07 (11)
1-pentanol	56	1.70	13.9	1.407	0.57		0.586	24.13	3.83	18.35	3.15	1.80	1.60	2.07 (13)
N-methylformamide	57	3.86	182.4	1.447	0.72		0.722	23.99	3.89	17.99	3.24	2.10	1.69	2.19 (15)
ethylene glycol	58	2.31	37.7	1.431	0.67	0.92	0.790	23.54	3.93	17.62	3.12	2.50	1.80	2.17 (30)
formamide	59	3.37	111.0	1.447	0.71	0.97	0.775	23.49	3.93	17.72	3.16	2.60	1.71	2.02 (17)

[a] Solvents are sorted into three catagories: "simple" dipolar solvents (nos. 1−25), nondipolar solvents (nos. 31−44), and hydrogen-bond-donating solvents (nos. 51−59). "HMPA" and "1,1,2-TCTF ethane" denote hexamethylphosphoramide and 1,1,2-trichlorotrifluoroethane, respectively. Except for fluoroform and carbon dioxide, all solvents are liquids at room temperature. For the former solvents, pressures and temperatures (∼35 °C) were chosen to provide near-liquid densities (shown in parentheses in units of g/cm^3). [b] Dipole moments (μ [D], taken mainly from measurements in benzene solution), static dielectric constants (ϵ_0), and refractive indices (n_D) are for 25 °C and were taken from the compilations in: Riddick, J. A.; Bunger, W. B.; Sakano, T. K. *Organic Solvents*; Wiley: New York, 1986). $F(\epsilon_0,n)$ are the reaction field factors defined by eq 1. The values of the solvatochromic polarity π^* are from ref 9, and E_T^N values are from ref 10. [c] $\bar{\nu}_{abs}$ and $\bar{\nu}_{em}$ are the average (first moment) frequencies of the (lowest frequency) absorption and emission bands of C153. Γ_{abs} and Γ_{em} are the full widths at half-maximum of these bands. δ_0 and Γ_{inh} are the parameters that characterize the inhomogeneous line broadening function used to relate the spectrum in a given solvent to that in the reference noninteracting solvent, 2-methylbutane. δ_0 and Γ_{inh} are respectively the shift and full width of the Gaussian function used to represent this line-broadening function. (See refs 5 and 6 for details.) All frequencies are in units of 10^3 cm^{-1}. [d] Estimates of the magnitude [10^3 cm^{-1}] of the time-dependent Stokes shift $\Delta\nu = \nu(0) - \nu(\infty)$ determined from the difference between the frequencies of "time-zero" spectra and steady-state spectra. In determining these frequencies, we used an average of the first-moment frequencies and the frequencies of the upper frequency half-height points of the spectra. For nondipolar solvents this procedure is more accurate than using the first-moment frequencies alone, as was done in ref 5. The numbers in parentheses indicate the estimated uncertainties in the final digits of these Stokes shifts. Because C153 undergoes an excited-state reaction in carbon tetrachloride, the value of $\Delta\nu$ listed for this solvent was estimated from the correlation between $\Delta\nu$ and Γ_{inh}.[7]

way that they result in a net zero dipole moment. This difference between the two solvents leads to vastly different reaction field factors, 0.44 in THF versus 0.03 in dioxane. Despite this difference, the nuclear reorganization energies measured by the C153 probe are nearly identical. At an atomic level, one imagines the mechanisms underlying the nuclear polarization response in both of these solvents to be nearly the same. In either case the response to the $S_0 \rightarrow S_1$ transition probably entails both rotational and translational motions that on average serve to bring nearby local dipoles of solvent molecules into closer proximity and better alignment with the local electric fields produced by the solute. Since these local

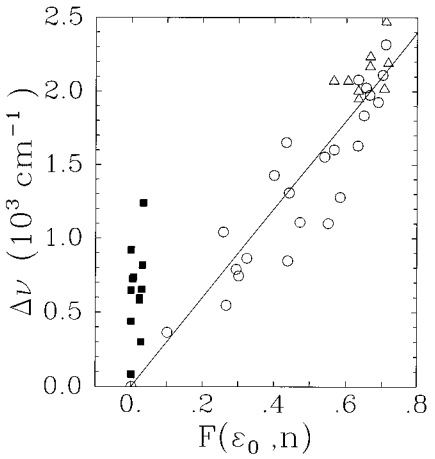

Figure 2. Stokes shift magnitudes $\Delta\nu$ plotted as a function of the reaction field factor $F(\epsilon_0,n)$ defined by eq 1. Simple dipolar solvents are shown as circles, hydrogen-bond-donating solvents as triangles, and nondipolar solvents as filled squares. The line represents the least-squares fit of the open symbols to the proportionality $\Delta\nu = (3.0 \times 10^3$ cm$^{-1})F(\epsilon_0,n)$ [correlation coefficient $R = 0.94$, for $n = 34$ solvents].

fields decay rapidly with distance from the solute, one does not expect full cancellation for a solvent molecule such as dioxane, whose opposing bond dipoles are separated by a distance comparable to the dimensions of the solute. (For example, modeling C153 as a spherical cavity dipole of radius 3.9 Å, for a radial alignment of the two O atoms in dioxane, the r^{-3} distance dependence of dipole−dipole interactions produces about a 3:1 ratio between the interactions energies of the two bond dipoles in this solvent molecule.) It is therefore not surprising that the reorganization energies are comparable in THF and dioxane. One should anticipate that any molecule that contains significantly polar bonds, whether it has a net dipole moment or not, might lead to significant electrostatic solvation energies. These energies are not accounted for in continuum models that employ only infinite-wavelength properties such as ϵ_0.

In addition to the more obvious source of dynamic Stokes shifts, modulation of the interactions between the *permanent* charge distributions of the solute and solvent, it should be noted that nuclear motions can also change interactions related to the electronic polarizabilities of the solvent and solute. For example, an increase or decrease in the density of a completely nonpolar solvent in the neighborhood of a solute should lead to a nonzero contribution to the Stokes shift, since such a change should modulate induced-dipole interactions between a solute and solvent. One therefore cannot automatically assume that only the permanent charge distributions are important in the Stokes shifts being observed. However, the data in Table 1 indicate that the electronic polarizability of the solvent does not play an important role in the Stokes shifts of C153 measured here. Thus, the Stokes shifts measured in carbon disulfide and perfluorohexane, solvents whose electronic polarizabilities differ by a more than a factor of 2,[11] are nearly identical to one another. Furthermore, the shifts in both of these solvents are zero to within the ± 100 cm^{-1} uncertainty limits of our measurements. We also note that in the case of *s*-tetrazine studied by Berg and co-workers,[12] where electronic polarizability effects are presumably dominant, the Stokes shifts observed in the solvents perfluorohexane and hexane were only 45 and 70 cm^{-1}, respectively. If, as seems reasonable, the contribution of solvent electronic polarizability is comparable in C153 and tetrazine, in C153, it represents a much smaller effect than the contributions due to permanent charge moments. As we will show in section V, the contributions of the permanent charge distributions of solvent molecules alone are sufficient to explain the shifts observed in this highly polar solute.

Before concluding the present section, it is instructive to compare the Stokes shifts observed here to two of the most popular empirical scales of solvent polarity, the π^*[9] and E_T^{N}[10] scales. Both of these commonly used measures of solvent "polarity" are based on solvatochromic shifts in the absorption spectra of particular indicator molecules: 4-nitroanisole in the case of the π^* scale and betaine "no. 30" in the case of the E_T^N scale. The individual absorption and emission frequencies of C153 (Table 1) show a high degree of correlation with both of these polarity scales, especially when hydrogen-bonding solvents are excluded. Linear regressions performed with the combined dipolar and nondipolar data in Table 1 yield

$$\bar{\nu}_{\text{abs}}\,[10^3\text{ cm}^{-1}] = 25.776 - 2.103\pi^* \quad (R = 0.97,\ n = 36)$$

$$\bar{\nu}_{\text{em}}\,[10^3\text{ cm}^{-1}] = 21.294 - 3.247\pi^* \quad (R = 0.93,\ n = 36)$$

and

$$\bar{\nu}_{\text{abs}}\,[10^3\text{ cm}^{-1}] = 25.629 - 4.032E_T^N \quad (R = 0.87,\ n = 33)$$

$$\bar{\nu}_{\text{em}}\,[10^3\text{ cm}^{-1}] = 21.244 - 7.199E_T^N \quad (R = 0.95,\ n = 33)$$

Addition of the hydrogen-bonding solvents from Table 1 degrades these fits significantly. In this case the correlation coefficients (R) are reduced to 0.94, 0.87, 0.84, and 0.91, in the above order. These regressions indicate that, at least for non-hydrogen-bonding solvents, the absorption frequencies of C153 are much better correlated to the π^* scale than to the E_T^N scale. In contrast, the E_T^N scale does a slightly better job of correlating the emission frequencies. This difference is best understood after we consider the Stokes shift magnitudes, which roughly speaking reflect the *differences* between absorption and emission frequencies.

Figures 3 and 4 show the Stokes shifts of C153 plotted against the π^* and E_T^N solvent polarities. The lines drawn in these figures are the fits to the data in Table 1 excluding the hydrogen-bonding solvents:

$$\Delta\nu\,[10^3\text{ cm}^{-1}] = 2.034\pi^* \quad (R = 0.73,\ n = 36)$$

and

$$\Delta\nu\,[10^3\text{ cm}^{-1}] = 4.803E_T^N \quad (R = 0.92,\ n = 33)$$

The first noteworthy feature of these data is that the nondipolar solvents (filled squares) do not stand out as being anomalous as they did when the reaction field factor $F(\epsilon_0,n)$ was used as a measure of the solvent polarity. Since both of the empirical polarity scales are based on solvation of a molecular solute, they do not make the mistake of categorizing as "nonpolar" all solvents which lack a net dipole moment. However, the two scales perform very differently when it comes to correlating the observed Stokes shifts of C153. On the basis of the good fit of the present data to the E_T^N scale, one can state that this polarity indicator, at least in non-hydrogen-bonding solvents, provides a good quantitative measure of the nuclear reorganization energies associated with dipolar solvation processes. The π^* scale, on the other hand, provides a rather poor measure. The difference in predictive ability of these two scales as regards the Stokes shifts reflects the differential sensitivity of the two scales to the electronic polarizability of the solvent. It is well-known that the π^* scale measures a blend of solvent "polarity and polarizability" [9,13] or in our language both the polarizability associated with rotation and translation of the permanent charge

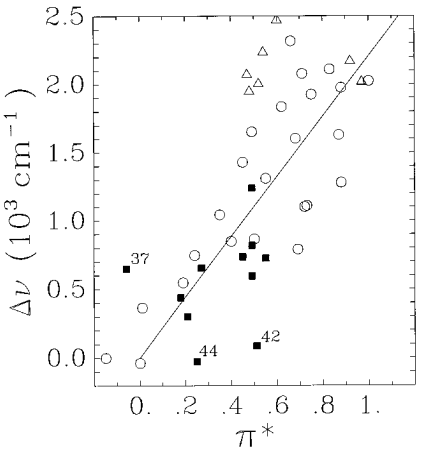

Figure 3. Stokes shift magnitudes $\Delta\nu$ plotted as a function of the solvatochromic polarity parameter π^*. Simple dipolar solvents are shown as circles, hydrogen-bond-donating solvents as triangles, and nondipolar solvents as filled squares. The line represents the least-squares fit of the simple aprotic and nondipolar data to the proportionality $\Delta\nu = (2.03 \times 10^3\ \mathrm{cm}^{-1})\pi^*$ [$R = 0.73$, $n = 36$]. The numbers refer to individual solvents as listed in Table 1: no. 37 = carbon dioxide, no. 44 = tetrachloroethylene, and no. 42 = carbon disulfide.

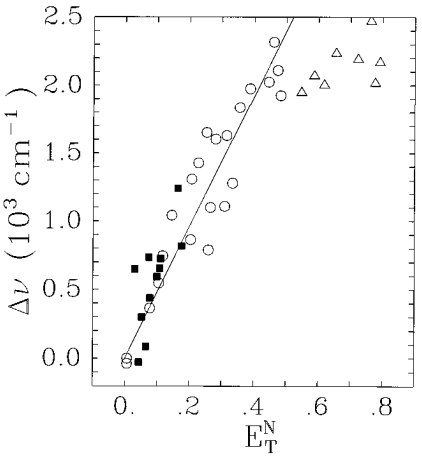

Figure 4. Stokes shift magnitudes $\Delta\nu$ plotted as a function of the solvatochromic polarity parameter E_T^N. Simple dipolar solvents are shown as circles, hydrogen-bond-donating solvents as triangles, and nondipolar solvents as filled squares. The line represents the least-squares fit of the simple aprotic and nondipolar data to the proportionality $\Delta\nu = (4.80 \times 10^3\ \mathrm{cm}^{-1})E_T^N$ [$R = 0.92$, $n = 33$].

distributions of solvent molecules as well as their "instantaneous" electronic polarizability. Thus, the widely different electronic polarizabilities of the solvents perfluorohexane (off scale in Figure 3) and carbon disulfide (no. 42) lead to very different values of π^*: -0.45 versus $+0.51$. Since the Stokes shifts of C153 are relatively unaffected by this part of the solvent response, its presence in the π^* scale is detrimental to its use in correlating these shifts and presumably other nuclear reorganizatiuon energies of this sort. The E_T^N scale, in contrast, appears to be relatively insensitive to solvent polarizability and thus is better able to correlate such reorganization energies.

This difference between the two scales, as well as the fact that individual absorption and emission shifts in C153 are better correlated to different empirical scales, can be rationalized in the following manner. On general grounds one expects that the relative importance of nuclear versus electronic contributions to the spectral shifts should increase with the polarity of the originating state of the transition.[5,14] The reason that the E_T^N scale better represents the purely nuclear reorganization energy measured by the Stokes shifts of C153 than does the π^* scale is that the absorptive transition in the betaine (E_T^N) probe involves a *decrease* in solute polarity (negative solvatochromism) whereas the 2-nitroanisole probe (π^*) *increases* in polarity upon absorption (positive solvatochromism). Similarly, the absorption frequency of C153 contains relatively more contribution from solvent electronic polarizability than does the emission frequency because the excited state of C153 is much more polar than the ground state. Thus, there is a better correlation between the absorption frequency of C153 and the π^* polarity and between its emission frequency and the E_T^N polarity scale.

IV. Solvent Molecule Charge Distributions

In this and the following section we will show how the Stokes shifts of C153 in both dipolar and nondipolar solvents can be understood in terms of interactions between the permanent charge distributions of solvent molecules and the change in the charge distribution of C153 upon excitation. We begin by considering the electrostatic properties of a number of the solvents listed in Table 1. Since information on the charge distributions (other than dipole moments) is relatively scarce, we will use the results of *ab initio* calculations for this purpose.

Ab initio calculations for all solvents were carried out at the RHF level with full geometry optimization in the 6-31G* basis set using the Gaussian 94 program package.[15] This level of calculation was chosen because previous studies have shown that it provides reliable estimates for electrostatic properties of molecules.[16,17] Table 2 provides a summary of the dipole moments and quadrupole tensor components of solvent molecules derived from these calculations, along with experimental values of these quantities where available.[18] Before comparing to experiment, some comment is necessary on the definition of the quadrupole components listed here. The Gaussian program outputs primitive quadrupole (and higher multipole) moments of the form[20]

$$\vec{\vec{\Theta}} = \sum_i q_i \vec{\mathbf{r}}_i \vec{\mathbf{r}}_i \tag{2}$$

where q_i represents the charge at position $\vec{\mathbf{r}}_i$. (Calculations are actually performed for the continuous distribution of charge implied by the wave function, but we show the discrete representations of $\vec{\vec{\Theta}}$ and $\vec{\vec{\mathbf{Q}}}$ here for simplicity.) Rather than employing these numbers directly, in Table 2 we report the traceless "standard" form[21]

$$\vec{\vec{\mathbf{Q}}} = {}^1/_2 \sum_i q_i (3\vec{\mathbf{r}}_i \vec{\mathbf{r}}_i - \mathbf{r}_i{}^2 \vec{\vec{\mathbf{1}}}) \tag{3}$$

In addition, the origin for the calculation of the quadrupole moment tensor assumed by the Gaussian program is the center of nuclear charge. For dipolar molecules (where the quadrupole moment depends on choice of origin), we transformed the quadrupole tensor to coincide with the molecular center of mass, since the latter is the origin used in most experiment determinations of $\vec{\vec{\mathbf{Q}}}$.

Comparisons between the calculated and observed magnitudes of the total dipole moments and quadrupole components of these molecules are provided in Figure 5. One sees from Figure 5A that there is reasonable agreement between the observed and calculated dipole moments for all molecules except for dimethyl sulfoxide (no. 4, DMSO). In the case of DMSO the calculated value (5.75 D) is 45% too high, perhaps due to an inadequate treatment of the expanded valence of the sulfur atom in DMSO. For all of the other molecules we find that the 6-31G* calculations overestimate the observed dipole moments by an

TABLE 2: Results of *ab Initio* (6-31G*//6-31G*) Calculations

		calculated values[a]									experimental values[b]				
molecule	no.	orien	sym	μ (D)	Q_{xx} (D Å)	Q_{yy} (D Å)	Q_{zz} (D Å)	Q_{xy} (D Å)	$\langle Q \rangle$ (D Å)	ESP	q_{max}	μ (D)	Q_{xx} (D Å)	Q_{yy} (D Å)	Q_{zz} (D Å)	method [ref]
acetonitrile	1	*Z*	C_{3v}	4.04	1.24	1.24	−2.49	0.00	2.49	N	−0.51	3.92			−1.8(1.2)	MA [*a*]
dimethyl sulfoxide	4	*YZ*	C_{2v}	5.75	−0.83	8.32	−7.49	0.00	9.17	O	−0.54	3.96				
nitromethane	6	*YZ*1	C_s	4.02	2.56	2.86	−5.42	−0.12	5.42	O	−0.48	3.46	2.2(4)	2.4(2)	−4.6(2)	MA [*b*]
acetone	7	*YZ*	C_{2v}	3.12	2.03	2.67	−4.69	0.00	4.71	O	−0.58	2.93	1.82(15)	2.77(13)	−4.59(10)	MA [*c*]
methyl acetate	8	*I*	C_s	2.00	0.58	−8.50	7.92	3.68*	10.41	O	−0.62	1.72				
fluoroform	11	*Z*	C_{3v}	1.70	−1.90	−1.90	3.81	0.00	3.81	F	−0.22	1.65			4.87(2); 4.5	MBER [*d*], DSV [*e*]
tetrahydrofuran	13	*YZ*	C_{2v}	1.96	1.28	3.90	−5.17	0.00	5.39	O	−0.53	1.75				
benzonitrile	14	*YZ*	C_{2v}	4.85	−1.55	13.54	−11.99	0.00	14.82	N	−0.47	4.14				
dichloromethane	15	*YZ*	C_{2v}	1.99	0.70	−4.12	3.43	0.00	4.41	H	+0.24	1.62				
1,2-difluorobenzene	16	*YZ*	C_{2v}	2.84	−4.38	4.72	−0.34	0.00	5.27	F	−0.20	2.46	−3.4(3)	7.0(2)	−3.6(3)	MA [*b*]
1,3-difluorobenzene	18	*YZ*	C_{2v}	1.66	−3.04	−5.08	8.12	0.00	8.21	H	+0.25	1.51	−2.6(1.3)	−5.0(9)	7.6(1.0)	MA [*f*]
chloroform	20	*Z*	C_{3v}	1.35	−1.43	−1.43	2.85	0.00	2.85	H	+0.30	1.04				
cyclohexane	25	*Z*	D_{3d}	0	−0.32	−0.32	0.65	0.00	0.65	H	+0.02	0			0.9(3)	DLS + CM + IB [*g*]
1,4-dioxane	31	*YZ*2	C_{2h}	0	−0.01	−9.62	9.63	−3.11	11.68	O	−0.44	0			⟨4.5⟩	FIR [*h*]
1,2,4,5-TFbenzene	32	*YZ*2	D_{2h}	0	3.74	−12.97	9.24	0.00	13.36	H	+0.27	0				
1,4-difluorobenzene	33	*YZ*2	D_{2h}	0	−2.18	12.46	−10.28	0.00	13.31	F	−0.22	0			⟨3.9⟩	FIR [*h*]
1,4-xylene	34	*YZ*1	C_{2h}	0	−7.67	4.38	3.29	0.20	7.69	H	+0.17	0				
benzene	35	*Z*	D_{6h}	0	4.17	4.17	−8.35	0.00	8.35	H	+0.14	0			−8.7(5); −8.5(1.4)	IB[*i*]; MA + SE[*j*]
hexafluorobenzene	36	*Z*	D_{6h}	0	−4.72	−4.72	9.43	0.00	9.43	F	−0.13	0			9.5(7)	IB [*i*,*k*]
carbon dioxide	37	*Z*	$D_{\infty h}$	0	2.73	2.73	−5.46	0.00	5.46	O	−0.45	0			−4.3(2)	MA; IB [*a*,*l*]
toluene	38	*YZ*1	C_s	0.27	−7.92	4.11	3.81	0.10	7.92	H	+0.16	0.38				
1,3,5-trifluorobenzene	40	*Z*	D_{3h}	0	−0.27	−0.27	0.54	0.00	0.54	H	+0.28	0			0.91(1)	IB [*k*]
carbon disulfide	42	*Z*	$D_{\infty h}$	0	−0.78	−0.78	1.56	0.00	1.56	S	−0.01	0			2.8(7); 4.3(3)	MA/CM[*m*]; IB[*n*]
perfluorohexane	43	*XY*	C_{2h}	0	−0.00	0.48	−0.48	−0.90	1.18	F	−0.17	0				
tetrachloroethylene	44	*YZ*2	D_{2h}	0	−1.45	1.89	−0.44	0.00	1.97	Cl	−0.02	0				
methanol	51	*I*	C_1	1.87	−1.42	1.38	0.03	3.29*	4.13	O	−0.69	1.68				
ethanol	52	*I*	C_s	2.02	0.13	4.48	−4.60	−1.69*	5.60	O	−0.74	1.71				
formamide	59	*I*	C_s	4.10	−2.40	3.29	−0.89	1.51*	3.83	O	−0.59	3.71	−3.1(8)	3.4(4)	−0.3(5)	MA [*a*]
water	60	*YZ*	C_{2v}	2.20	−2.26	2.39	−0.13	0.00	2.69	O	−0.80	1.86	−2.50(2)	2.63(2)	−0.13(3)	MA [*a*]
dimethyl ether	61	*YZ*	C_{2v}	1.61	−0.94	3.28	−2.34	0.00	3.38	O	−0.45	1.30	−1.3(1.0)	3.3(6)	−2.0(5)	MA [*a*]
ammonia	62	*Z*	C_{3v}	1.92	1.32	1.32	−2.64	0.00	2.64	N	−1.08	1.47			−2.32(7)	MA [*a*]
coumarin 153[c]		*XY*1	C_1	6.81	17.16	−19.04	1.89	5.70	22.02	O	−0.61	6.55				
S_0[MNDO]		*XY*1	C_1	6.98	18.17	−17.41	−0.76	−5.10	21.50	O	−0.54	6.55				
$\Delta q(S_1-S_0)$[MNDO]		*XY*1	C_1	7.95	1.27	−1.03	−0.24	2.10	2.86			∼8				

[a] All coordinate systems have their origins at the molecular center of mass. Orientations are designated as follows: *Z* (*z* axis is the principal axis), *YZ* (molecule lies in the *YZ* plane with *z* axis as principal axis), *YZ*1 (*YZ* with C−N {no. 6} or Me {no. 34 and no. 38} along *y* axis), *YZ*2 (*YZ* with O {no. 31}, H {no. 33}, or C {no. 44} atoms along *z* axis), *XY* (molecule lies in the *XY* plane with *z* axis as principal axis), *XY*1 (molecule lies in the *XY* plane), or *I* (molecule in principal inertial axes frame with $I_{xx} > I_{yy} > I_{zx}$). For molecules in orientation *I*, the reported Q_{xy} values denoted with an asterisk are actually Q_{yz} values. $\langle Q \rangle$ is the effective axial quadrupole moment defined by eq 4. "ESP q_{max}" lists the atom type and the charge on the most highly charged atom on the periphery of the molecule. [b] Dipole moments of the solvent molecules listed here are gas phase values obtained from: *Landolt-Börnstein, Numerical Data and Functional Relationships in Science and Technology, New Series*; Springer-Verlag: Berlin, 1994; Group II, Vol. 19. Values listed for C153 are from refs 26 and 30. Quadrupole moments were measured by the following experimental methods (abbreviations after Gray and Gubbins[19]): CM (Cotton−Mouton effect measurement), DLS (depolarized light scattering), DSV (dielectric second virial coefficient), FIR (far-infrared absorption), IB (field-gradient induced birefringence), MA (magnetizability anisotropy via microwave spectroscopy), MBER (molecular beam electric resonance spectrometry), SE (semiempirical calculation). Where available, uncertainties are shown in parentheses. The values for dioxane and 1,4-difluorobenzene (in ⟨ ⟩ are only estimates of the overall magnitude of the quadrupole moment tensors for these molecules. References to the original papers are contained in ref 18. [c] The first row lists results for the ground state of C153 obtained from 6-31G** calculations. The second row ("S_0[MNDO]") are ground-state values calculated from MNDO/CI calculations scaled by the empirical factor 1.24. (See text.) The third row ("$\Delta q(S_1-S_0)$[MNDO] are the charge difference obtained from MNDO/CI calculations again scaled by a factor of 1.24.

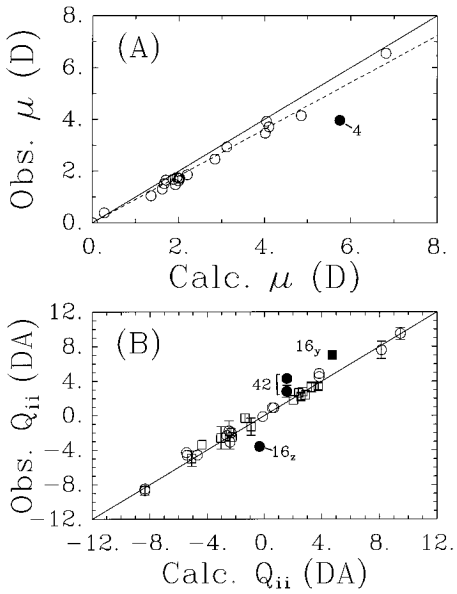

Figure 5. Comparison of calculated and experimental values of (A) the dipole moments and (B) the quadrupole tensor components of a variety of solvents. The solid lines in both panels is the line of equality. The dashed line in the top panel is the best fit of the data to the relation $\mu(\text{obs}) = 0.90\mu(\text{calc})$ [$R = 0.99$, $n = 20$]. The filled point (no. 4) in panel A is the result for dimethyl sulfoxide, which was excluded from the fit. The solvents identified by number in the bottom panel are no. 16 = 1,2-difluorobenzene ("*y*" and "*z*" refer to Q_{yy} and Q_{zz}, respectively) and no. 42 = carbon disulfide. See text and Table 2 for further details.

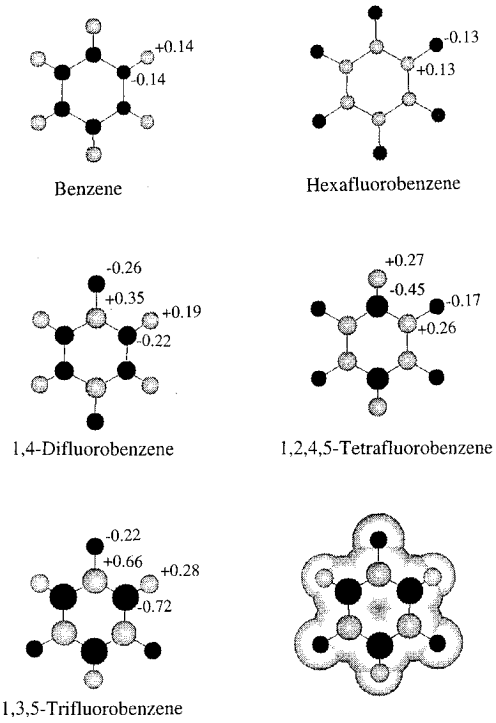

Figure 6. Schematic illustration of the ESP-fitted charges determined for some substituted benzenes. The volumes of the spheres represent the charge at a given atomic site. Dark spheres represent negative charge and light spheres positive charge. Some charges (in au) are also indicated. The figure in the lower right shows the van der Waals surface of 1,3,5-trifluorobenzene, which is representative of those used in the binary interaction calculations.

average of 10%, as indicated by the dashed line in Figure 5A (slope = 0.90, $R = 0.99$, $n = 20$). This small systematic error for this level of calculation is expected on the basis of many previous comparisons of this sort.[16] The quadrupole components are compared in Figure 5B. Taking into account the experimental uncertainties involved, the calculations reproduce nearly all of the available quadrupole moment data to within ±1 D Å. The main exceptions (filled symbols) are CS_2 (no. 42) and 1,2-difluorobenzene (no. 16). CS_2 has been known to be a troublesome case for some time now.[22] In the case of 1,2-difluorobenzene, the unusually large deviation from the calculated values of Q_{yy} and Q_{zz} suggests a possible experimental error. Thus, with the exceptions of the two sulfur-containing compounds, measured electrostatic properties appear to be reproduced to about the 10−20% level in these calculations. This level of accuracy is sufficient for our purposes.

In order to gain some appreciation for the nature of the charge distributions of the various solvent molecules studied, as well as to facilitate the calculations described in the next section, electrostatic potential (ESP) fitting of the *ab initio* wave functions was performed. For each solvent molecule, the full charge distribution implied by the nuclear charges plus electronic wave function was fit to the set of atom-centered point charges that best reproduces the electrostatic potential outside of the van der Waals surface of the molecule. The fitting was performed using the Merz−Singh−Kollman scheme in Gaussian 94[23] with the constraint that the fitted charges reproduce the expectation value of the dipole moment. Although no such constraints were placed on the quadrupole moments, excellent agreement was observed between the expectation values of the quadrupole components and those obtained from the ESP-fitted charges. (We observed an average absolute deviation of <0.3 D Å for the 110 nonzero quadrupole components in Table 2.) Thus, although more sophisticated representations of molecular charge distributions are available, the atom-centered point charges generated via ESP fitting are adequate to model at least the quadrupole moments of the distributions to within the accuracy of our *ab initio* calculations.

Figure 6 illustrates the nature of the charge distributions so determined for five fluorinated benzene solvents. These diagrams provide useful perspective on the meaning of the quadrupole moments of these molecules. For example, we note that the magnitudes of the atomic charges in both benzene and hexafluorobenzene correspond to sizable bond dipole moments: 0.72 D for the C−H bonds in benzene and −0.81 D for the C−F bonds in hexafluorobenzene. These comparable bond polarities lead to comparable quadrupole moments (Q_{zz}) in the two molecules, −8.3 and +9.4 D Å, respectively. The sign difference between Q_{zz} in the two molecules reflects the opposite directionality of the bond dipoles, with the negative value for benzene resulting from fact that the outer ring of charge is positive. (In benzene-like cases, eq 3 becomes $Q_{zz} = -{}^1/_2\sum_j q_j r_j^2$, where r_j is the distance from the center of the ring to atom j.) Like the benzene/hexafluorobenzene pair, the 1,4- and 1,2,4,5-substituted benzenes are seen to be approximate "charge inverses" of one another. Note, however, that the individual bond dipoles in these molecules are significantly larger than in the former cases, resulting in average quadrupole moments ($\langle Q \rangle$, see below) that are substantially larger than in benzene or hexafluorobenzene. This enhancement of the individual bond dipoles can be viewed as a type of inductive effect, which has long been recognized to spoil simple bond-additivity schemes for calculating dipole moments.[24] In the case of 1,3,5-trifluorobenzene this effect is particularly pronounced. However, while 1,3,5-trifluorobenzene exhibits the largest charge separation within this series of molecules, the near balance of (opposite) charges on the H and F atoms results in the quadrupole moment of this molecule being close to zero. Just as in the case of the zero dipole moment of the benzene

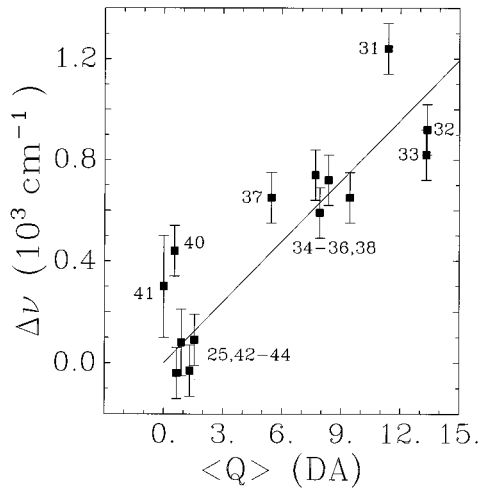

Figure 7. Stokes shift magnitudes $\Delta\nu$ plotted as a function of the effective quadrupole moments of nondipolar solvents. The numbers indicate the solvent identities as listed in Table 1. The line indicates the best fit to the data: $\Delta\nu = 0.0796\langle Q\rangle$ [$R = 0.85$, $n = 14$].

molecule, the symmetry in 1,3,5-trifluorobenzene imposes a near-zero quadrupole moment event though its individual bonds are markedly polar.

We now consider how the electrostatic properties just calculated are related to the magnitude of the Stokes shifts (nuclear reorganization energies) that the various solvents produce in C153. It is clear from Figure 6 that, although molecules such as the fluorinated benzenes are not dipolar, all of these molecules contain significantly polar bonds and that these bond polarities should result in significant multipole moments of higher than dipolar order. It therefore seems natural to attribute the Stokes shifts observed in such solvents to these higher-order multipole moments. If this assignment is correct, one would expect to find a simple relationship between the magnitude of the next higher multipole, the quadrupole moment, and the magnitudes of the Stokes shifts observed in nondipolar solvents. To examine this possible relationship, it is convenient to reduce the quadrupole tensor $\overleftrightarrow{\mathbf{Q}}$, which is a traceless, symmetric, second-rank tensor, to a single quantity expressive of its overall magnitude. For this purpose we use the so-called "effective axial quadrupole moment" $\langle Q\rangle$ used by Gray and Gubbins[25],

$$\langle Q\rangle^2 \equiv {}^2/_3\overleftrightarrow{\mathbf{Q}}:\overleftrightarrow{\mathbf{Q}} \tag{4}$$

For a molecule with true axial symmetry (one with a 3-fold or higher rotation axis) this definition yields $\langle Q\rangle = |Q_{zz}|$, in keeping with the conventional designation of Q_{zz} as *the* quadrupole moment.

Figure 7 illustrates the relationship between the Stokes shift of C153 and magnitude of $\langle Q\rangle$ for the nondipolar solvents examined. A general trend of increasing Stokes shift with increasing quadrupole size is obvious. With few exceptions, the ordering of solvents with respect to $\langle Q\rangle$ is as anticipated for solvation dominated by contributions from solvent quadrupolar interactions. Thus, these solvents can be grouped into those with small ($\langle Q\rangle \leq 2$; nos. 25, 40−44) intermediate ($2 \leq \langle Q\rangle \leq 10$; nos. 34−38), and large ($10 \leq \langle Q\rangle$; nos. 31−33) quadrupole moments, and the Stokes shifts generally follow this same grouping. But, the correlation between $\Delta\nu$ and $\langle Q\rangle$ is far from perfect. For example, one notes that dioxane (no. 31) shows an unexpectedly large Stokes shift compared to the other (mainly fluorinated benzene) solvents. The difference between dioxane and benzene solvents probably reflects the difference in charge localization in the two types of molecules, and this difference is not accounted for in $\langle Q\rangle$. In addition, the solvents 1,3,5-trifluorobenzene (no. 40) and carbon tetrachloride (no. 41) show substantial Stokes shifts even though their quadrupole moments are either nearly or identically zero. This latter observation is not surprising, especially in the case of 1,3,5-trifluorobenzene, where, as just discussed, the individual bond polarities are even larger than in the other fluorobenzenes. Thus, although 1,3,5-trifluorobenzene and carbon tetrachloride have neither dipole nor (significant) quadrupole moments, one expects higher-order (octapolar) moments of the charge distribution to still be effective for solvation.

V. Charge Distribution of C153 and Binary Interaction Calculations

The correlation illustrated in Figure 7 provides reasonably convincing evidence that the origin of the nuclear reorganization energies of C153 in nondipolar solvents lies in interactions with the higher-order multipole moments of the solvent. In this section we expand on this idea and show that these reorganization energies in both dipolar and nondipolar solvents can in fact be understood on an equal footing by considering the electrostatic interactions between the solute and the complete permanent charge distribution of a single solvent molecule.

To begin with, we must consider the charge distribution of the solute C153. To this end we have performed *ab initio* and semiempirical calculations for the ground (S_0) and excited (S_1) states of this solute. The *ab initio* calculations of the ground state of C153 were performed in a manner identical to the solvent calculations described in the last section, with the exception that the geometry was fixed at the one determined by semiempirical calculations. The dipole moment calculated in this way, 6.8 D, is in good agreement with the value from experiment, 6.55 ± 0.01 D, in dioxane solution.[26] We anticipate similar accuracy for other aspects of the ground-state charge distribution, as was found for the smaller molecules discussed in section IV. Since the observed Stokes shift involves the transition $S_0 \leftrightarrow S_1$, modeling these shifts requires knowledge of the difference between the charge distributions in the S_0 and S_1 states. This difference ("Δq") distribution was obtained from semiempirical calculations with the MNDO Hamiltonian and a 10×10 CI calculation using the AMPAC program package.[27,28] Previous studies have shown that such calculations provide reasonable estimates of the properties of the first excited states of coumarins.[29] The MNDO-CI calculations yield an S_0 dipole moment of 5.6 D, somewhat smaller than the experimental and *ab initio* results. The S_1 dipole moment is calculated to be 12.0 D, which is also slightly smaller than the values of 14−16 D (depending on solvent) found experimentally.[30] In order to provide a convenient basis for calculation, electrostatic potential fits were also performed for both the *ab initio*[23a] and semiempirical wave functions.[23b] The charges so generated for the ground state using the MNDO-CI wave function were found to be in reasonably good agreement ($R = 0.89$ for $n = 34$) with the *ab initio* charges but with a regression coefficient of 1.24 rather than unity, i.e., q_i(*ab initio*) $= 1.24q_i$(MNDO-CI).[31,32] When this scaling factor is applied to the MNDO-CI charges, values of 6.98 and 14.9 D are obtained for the S_0 and S_1 dipole moments, in much closer agreement with both the *ab initio* and experimental values. Furthermore, after such scaling there is excellent agreement with the quadrupole tensor components calculated from these MNDO-CI charges and the *ab initio* wave function. (See the final two rows of Table 2.) For the charge differences that characterize the $S_0 \leftrightarrow S_1$ transition, we therefore

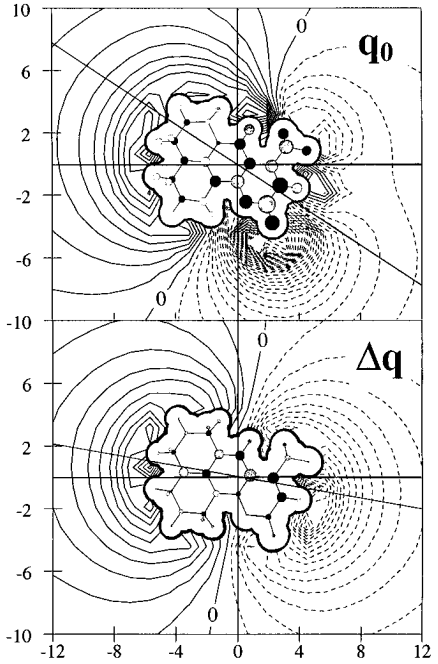

Figure 8. Charge distributions and electrostatic potentials corresponding to the ground (S_0) state "q_0" and to the difference between the S_1 and S_0 states "Δq". The ground-state charges are from 6-31G*//MNDO calculations, while the difference charges are from MNDO-CI calculations. (See text.) The molecular outline shows the van der Waals surface of the molecule used in the binary interaction calculations. Coordinates are in angstroms. The spheres at the atomic sites represent the ESP-fit charges. The lighter/darker spheres represent positive/negative charge, with the amount of charge being proportional to the volume of the sphere. (For purposes of calibration, the charge on the carbonyl oxygen atom is -0.61 au in the q_0 distribution and $+0.01$ in the Δq distribution.) The contour lines show the electrical potential spaced at intervals of 2 au. The solid and dashed contours represent positive and negative values, respectively. The diagonal lines show the direction of the dipole moments $\vec{\mu}(S_0)$ and $\Delta\vec{\mu} = \vec{\mu}(S_1) - \vec{\mu}(S_0)$. In both cases the positive end of the dipole lies in the upper left-hand quadrant.

employ the differences between the MNDO-CI calculations of S_0 and S_1 (at the S_0 geometry) scaled by the empirical factor of 1.24. For representing the S_0 interactions we employ the *ab initio* charges.

Figure 8 shows electrostatic potential maps for the ground-state charge distribution "q_0" (from the *ab initio* calculations) and the difference distribution, Δq. Superimposed on these maps are representations of the van der Waals surface of the molecule, the dipole moment directions, and the ESP-derived charges. The main feature of note in the ground state potential is the region of high negative potential near the carbonyl oxygen atom. The charge on this atom is calculated to be -0.61 au, and at close range, the potential in its vicinity looks like that of a small negative ion. Within the first solvation shell, the S_0 potential is therefore significantly distorted from that of a simple point dipole lying along the molecular dipole axis. Analysis of the "effective multipole moment" of the ground-state charge distribution, as was done in ref 4, shows that a dipolar solvent would sense this potential as being more comparable to that of a point quadrupole than a point dipole. In contrast, the difference potential looks very much like that of a pure point dipole. The difference $[\Delta\vec{\mu} = \vec{\mu}(S_1) - \vec{\mu}(S_0)]$ is of nearly the same magnitude as the ground-state dipole moment, but it is rotated from it by some 23°. The reason for the particularly simple appearance of the difference potential is that the $S_0 \rightarrow S_1$ transition in C153 mainly involves redistribution of electron density among the carbon atoms within the coumarin ring. There is very little redistribution of charge on any of the peripheral atoms such as the carbonyl oxygen. (For example, Δq for this atom is only calculated to be $+0.01$ au.) In keeping with the dipolar appearance of the potential, an effective multipole analysis of the Δq distribution shows that as far as a dipolar solvent is concerned, this solute perturbation is equivalent to that of a point dipole jump.

We now return to consideration of the solvation of C153. Suppose that the Stokes shifts observed with C153 are dominated by interactions between the solute ("Δq") distribution and the permanent charge distributions of the solvent molecules. If so, we should be able to reproduce the observed spectral shifts using the information on solute and solvent charge distributions presented above. To test this claim, we could perform computer simulations of C153 in model solvents constructed from the ESP fit charges together with some suitable representation of the nonelectrostatic interactions. We have in fact already performed such calculations for two solvents, acetonitrile and methanol.[4] These simulations involved equilibrium molecular dynamics simulations of ~256 solvent molecules interacting with the ground state of C153. From such simulations the Stokes shift can be calculated via the linear response relation[4,33]

$$\Delta\nu_{0\leftrightarrow 1} = (hc/kT)\langle\delta\Delta\nu^2\rangle^{(0)} \qquad (5)$$

where hc is Planck's constant times the speed of light and kT is the thermal energy. This expression relates the magnitude of the Stokes shift observed subsequent to the $0 \leftrightarrow 1$ transition to the fluctuations in the frequency of this transition ($\delta\Delta\nu$) for a system in equilibrium with the initial state ("0"). The frequencies $\Delta\nu$ are assumed to result from the Coulombic interactions between the permanent charge distributions of solvent molecules and the difference charges Δq. Using the MNDO-CI values for the Δq distribution and simplified three-site models for the solvents,[34] we obtained values of 2640 and 2950 cm^{-1} for the Stokes shifts in acetonitrile and methanol, respectively.[35] These values compare quite favorably to the experimental values of 2320 and 2470 $\pm$ 100 cm^{-1} in these solvents. The ability to closely model the experimental values in these two cases lends considerable confidence to the idea that the Stokes shifts observed here do indeed arise primarily from interactions between the solute difference distribution and the permanent charge distributions of solvent molecules.[36]

To perform the same sorts of molecular dynamics simulations on the variety of solvents of interest here would be an arduous task. We have instead chosen to perform a less rigorous and less time-consuming test, using simulations of the interactions between C153 and a *single solvent molecule*. Motivated by the idea that the orientations of most solvent molecules within the first solvation shell of a large solute such as C153 should be nearly isotropic,[37] we simply sampled the energetics of randomly oriented solute−solvent pairs. This was accomplished by bringing a randomly oriented solvent molecule up to van der Waals contact with some randomly chosen site on the surface of the solute. The Lennard-Jones parameters used for defining the molecular surfaces were obtained largely from Jorgensen's OPLS parameter set contained in the BOSS program,[38] while the electrostatic interactions were determined from the ESP fit atomic charges discussed above. For a given solute−solvent configuration, the total interaction energy with the ground state of C153, U_{tot}, the electrostatic component of this energy E_{el},

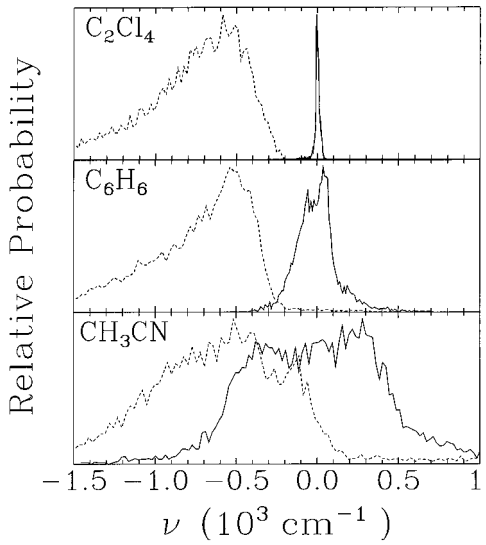

Figure 9. Distributions of the total (dashed curves) and the electrostatic component (solid curves) of the interaction energy between C153 and single solvent molecules of tetrachloroethylene, benzene, and acetonitrile. The distribution is sampled over 10 000 random orientations of the solute−solvent pairs at van der Waals contact (see text).

and the spectral shift, $\Delta\nu$, were calculated. The latter corresponds to the electrostatic energy of interaction with the "Δq" charge distribution. This random sampling process was repeated for 10 000 trials in order to adequately sample the energy and shift distributions.

The types of distributions generated in this manner are illustrated in Figure 9. The dashed curves are the total energy (U_{tot}) distributions while the solid curves are the electrostatic component of the interaction with the S_0 solute. (The distributions of the spectral shifts ($\Delta\nu$) happen to be very similar to the E_{el} distributions, due to the chance similarity of $\bar{\mu}(S_0)$ and $\Delta\bar{\mu}(S_1-S_0)$, and they have been omitted for the sake of clarity.) The total energy distributions for most solvents appear similar to those of tetrachloroethylene and benzene in Figure 9. In most solvents, the total solvation energy is largely determined by the Lennard-Jones rather the electrostatic interactions, and in the tetrachloroethylene and benzene cases the U_{tot} distribution largely reflects the distribution of Lennard-Jones interactions. For highly dipolar solvents the contribution of E_{el} to the total energy changes the shape of the distribution from one characteristic of the Lennard-Jones interactions to a more symmetric shape as in the acetonitrile case shown in Figure 9. In all of the solvents examined here the average Lennard-Jones interac-

TABLE 3: Results of Binary Interaction Calculations

									multipole decompositions (%)[c]									
		moments[a]			distribution characteristics[b]				E_{el}					$\Delta\nu$				
solvent	no.	μ (D)	$\langle Q\rangle$ (D Å)	$\mu/\langle Q\rangle$ Å^{-1}	$-U_{tot}$ (cm^{-1})	σ_{tot} (cm^{-1})	σ_{El} (cm^{-1})	$\sigma_{\Delta\nu}$ (cm^{-1})	tot.	*u*1	*u*2	*u*3	*u*4	tot.	*u*1	*u*2	*u*3	*u*4
acetonitrile	1	4.04	2.49	1.62	598	477	381	422	108	96	2	1	1	102	98	1	0	0
dimethylsulfoxide[d]	4	3.96	6.31	0.63	703	602	347	351	104	88	10	3	0	98	93	7	0	0
nitromethane	6	4.02	5.42	0.74	667	502	389	414	114	87	12	1	0	108	94	6	0	0
acetone	7	3.12	4.71	0.77	645	426	305	302	93	86	12	1	1	92	92	7	1	0
methyl acetate	8	2.00	10.41	0.19	705	413	249	240	117	41	54	2	3	100	54	45	1	0
fluoroform	11	1.70	3.81	0.45	492	290	193	197	127	75	22	3	0	113	87	13	1	0
tetrahydrofuran	13	1.96	5.39	0.36	645	347	190	193	88	72	26	2	0	89	81	18	1	0
benzonitrile	14	4.85	14.82	0.33	880	538	325	347	262	42	16	36	7	163	66	15	17	2
dichloromethane	15	1.99	4.41	0.45	620	348	201	204	126	78	19	2	1	114	86	13	1	0
1,2-difluorobenzene	16	2.84	5.27	0.54	797	437	214	219	220	46	12	30	13	140	77	9	12	2
1,3-difluorobenzene	18	1.66	8.21	0.20	798	422	166	146	229	25	29	33	13	162	47	31	19	3
chloroform	20	1.35	2.85	0.47	686	337	133	135	117	74	18	6	2	103	87	11	2	0
cyclohexane	25	0	0.65	0	684	285	11	9	124	0	89	0	11	111	0	96	0	4
1,4-dioxane	31	0	11.68	0	700	364	189	158	103	0	99	0	1	101	0	99	1	0
1,2,4,5-TFbenzene	32	0	13.36	0	813	439	176	160	190	0	67	0	33	122	0	91	0	9
1,4-difluorobenzene	33	0	13.31	0	795	428	175	150	196	0	70	0	30	133	0	89	0	11
1,4-xylene	34	0	7.69	0	833	425	136	110	191	0	79	0	21	120	0	95	0	5
benzene	35	0	8.35	0	772	405	165	134	191	0	80	0	20	124	0	96	0	4
hexafluorobenzene	36	0	9.43	0	825	444	178	148	225	0	76	0	24	132	0	94	0	6
carbon dioxide	37	0	5.46	0	452	284	189	150	114	0	99	0	2	106	0	100	0	0
toluene	38	0.27	7.92	0.03	800	410	142	117	196	1	72	7	20	122	2	88	5	5
1,3,5-trifluorobenzene	40	0	0.54	0	801	410	126	90	155	0	1	97	2	120	0	2	98	0
carbon tetrachloride	41	0	0	0	740	329	33	19	140	0	0	92	8	114	0	0	96	4
carbon disulfide	42	0	1.18	0	705	333	7	6	126	0	97	0	3	111	0	99	0	1
perfluorohexane	43	0	1.97	0	927	396	37	17	303	0	5	0	95	280	0	16	0	84
tetrachloroethylene	44	0	1.32	0	791	368	18	14	146	0	89	0	11	116	0	97	0	3
methanol	51	1.87	4.13	0.45	462	345	277	256	89	71	27	2	1	94	82	17	1	0
ethanol	52	2.02	5.60	0.36	535	347	247	242	92	62	32	5	1	91	76	23	2	0
formamide	59	4.10	3.83	1.07	563	527	457	486	110	86	7	6	1	104	95	4	2	0

[a] Dipole moments and effective axial quadrupole moments derived from *ab initio* calculations. See Table 3. [b] Characteristics of the energy and spectral shift distributions obtained from binary interaction calculations. U_{tot} is the mean of the distribution of interaction energies, and σ_{tot} is the standard deviation of this distribution. σ_{El} and $\sigma_{\Delta\nu}$ are the standard deviations of the distributions of the electrostatic interaction energy and of the spectral shift. The latter quantity is calculated as the interaction energy between the solvent molecule's charge distribution and the charge difference ("Δq") distribution of C153. [c] Decomposition of the E_{el} and $\Delta\nu$ distributions into contributions from different multipole moments of the full solvent-molecule charge distribution as described in the text. The labels "*uj*" denote interaction between the full solute charge distribution (q_0 for E_{el} and Δq in the case of $\Delta\nu$) and the *j*th moment of the solvent charge distribution. ($j = 1$ corresponds to dipole, 2 to quadrupole, etc.) The columns labeled "tot." are the ratios of the energies calculated from eq 6 (to fourth order in the solvent multipole expansion) to the energies calculated according to the full atom−atom interactions $\sigma^2(E_{el}^{mp})/\sigma^2(E_{el})$. The columns labeled "*uj*" are the relative contributions of the different multipole orders to the energy calculated via eq 6. In all cases the percentages listed here are comparisons of the standard deviations of the various distributions, normalized according to eq 7. [d] Since the *ab initio* calculations yielded values of the dipole moment of dimethyl sulfoxide that are in error by some 40%, the charges employed for calculations with this solvent were rescaled in order to match the magnitude of the experimental dipole moment.

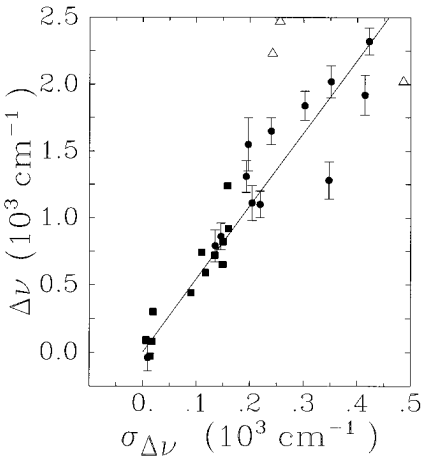

Figure 10. Stokes shift magnitudes $\Delta\nu$ plotted as a function of the width (standard deviation) of the frequency shift distribution, $\sigma_{\Delta\nu}$, calculated from randomly sampled solute−solvent distributions of the sort illustrated in Figure 9. The line drawn here is the best fit of the data shown as filled symbols (i.e., the data excluding the hydrogen-bonding solvents) to the proportionality $\Delta\nu = 0.54\sigma_{\Delta\nu}$ ($R = 0.94$, $n = 26$).

tion at randomly sampled contact configurations is on the order of −700 cm^{-1}. In contrast, such random sampling leads to an electrostatic interaction energy that averages to nearly zero in all cases, due to the exact or approximate charge-reversal symmetry of electrostatic interactions. However, the relative strength of the electrostatic interactions in different solvents is clearly revealed in the breadth of their E_{el} or $\Delta\nu$ distributions. In the tetrachloroethylene, benzene, and acetonitrile cases illustrated in Figure 9, the widths of the E_{el} distributions, as measured by their standard deviations (σ_{El}), are 7, 165, and 381 cm^{-1}, respectively. Thus, in the spirit of eq 5, we can use the widths of either the E_{el} or $\Delta\nu$ distributions to quantify the relative magnitudes of the electrostatic interactions of different solvents with C153. Values of these standard deviations are provided in Table 3.

The correlation between the widths of the spectral shift distributions ($\sigma_{\Delta\nu}$) derived from these binary interaction calculations and the Stokes shifts observed in the corresponding liquid solvents is shown in Figure 10. If one ignores the hydrogen-bonding solvents (open triangles), the correlation is rather remarkable ($R = 0.94$, $n = 26$). Virtually the same quality correlation is found using σ_{El} in place of $\sigma_{\Delta\nu}$. We take this high degree of correlation to these measures of electrostatic interaction strength as proof that the reorganization energies being measured *in all solvents* are predominantly due to interactions between C153 and the permanent charge distributions of solvent molecules. In the case of strongly dipolar solvents, these interactions can be well modeled by continuum dielectric formulas. In the case of nondipolar but quadrupolar solvents, the magnitude of the quadrupole moment serves to correlate the magnitude of the interactions. In more complicated cases such as dioxane or 1,3,5-trifluorobenzene, the full charge distribution of the solvent molecules must be considered for adequate modeling. Nevertheless, the underlying electrostatic origins of the Stokes shifts are the same in all cases.

It may seem surprising that the sort of random sampling of *pairwise* solute−solvent interactions performed here is sufficient to rationalize the reorganization energies observed in this wide range of solvents. After all, a characteristic feature of polar solvents is that important correlations exist between pairs of solvent molecules, and such correlations are completely neglected in the present calculations. These intersolvent correlations, which serve to "quench" the size of the solvation response,[39] should increase in relative importance as the size of the solvent−solvent interactions increases. Their neglect may account for the fact that the use of $\sigma_{\Delta\nu} = \sqrt{\langle\delta\Delta\nu^2\rangle}$ in Figure 10, rather than the $\langle\delta\Delta\nu^2\rangle$ suggested by eq 5, provides a more nearly linear relationship when used with these uncorrelated solvent calculations. It seems reasonable to expect that more sophisticated simulations, which at least approximately account for the effects of solvent−solvent correlations might enable one to make direct linear response estimates of the reorganization energies based on eq 5 and still avoid doing full molecular dynamics calculations of all of the solvents examined here. However, for now we will consider Figure 10 as sufficient proof that only the permanent charge distributions of solvent molecules are important in determining the observed Stokes shifts (nuclear reorganization energies) of the C153 probe.

To conclude this analysis, we consider decomposing the above distributions into contributions from different solvent multipole moments. To do so, we have evaluated the electrostatic interaction energies (E_{el}) and shifts ($\Delta\nu$) described above via a multipole expansion with respect to the solvent charge distribution. That is, while maintaining a fully atomic representation of the solute, the charge distribution of each solvent molecule was represented by a set of point multipoles placed at its center of mass, and the electrostatic interactions were recalculated to fourth (hexadecapole) order as

$$E_{el}^{mlt} = E_{ul} + E_{u2} + E_{u3} + E_{u4}$$

$$\Delta\nu^{mlt} = \Delta\nu_{ul} + \Delta\nu_{u2} + \Delta\nu_{u3} + \Delta\nu_{u4} \qquad (6)$$

The subscripts "*uj*" in these expressions denote the interaction of the full solute ("*u*") charge distribution (q_0 in the case of E_{el} and Δq in the case of $\Delta\nu$) and the *j*th-order multipole moment of the solvent. The formulas needed for calculating the various multipole components are summarized in the Appendix. The total solute−solvent interaction strength, as measured by the widths of the E_{el} and $\Delta\nu$ distributions, may then be approximately decomposed into contributions from different solvent multipoles by assuming that the widths are additive in quadrature,

$$\sigma^2(E_{el}) \cong \sigma^2(E_{el}^{mlt}) \equiv \sum_{j=1}^{\infty}\sigma_{u,j}^2(E_{el})$$

$$\sigma^2(\Delta\nu) \cong \sigma^2(\Delta\nu^{mlt}) \equiv \sum_{j=1}^{\infty}\sigma_{u,j}^2(\Delta\nu) \qquad (7)$$

The results of such a multipole decomposition are provided in Table 3. The columns labeled "tot." are the ratios $\sigma^2(E_{el}^{mlt})/\sigma^2(E_{el})$ of the variances in the energies calculated from the multipolar expansion to those calculated from the full atom−atom representation of all interactions. When the ground-state charge distribution of C153 is considered, one finds that this decomposition systematically overestimates the strength of the interactions (E_{el}) by an average of about 40%. The accuracy is better in the case of solvents interacting with the Δq solute charges ($\Delta\nu$ distribution). Here the values of $\sigma^2(\Delta\nu)$ are again too high, but only by an average of about 15%. The main source of the difference between $\sigma^2(E_{el}^{mlt})$ and $\sigma^2(E_{el})$ is the neglect of cross-terms in the expansion of E_{el}^2, predominantly negative terms arising from cross-correlations between E_{1u} and E_{3u} and between E_{2u} and E_{4u}, rather than errors resulting from truncating the multipole expansion at fourth order. We note that including these cross-terms does not appreciably affect the relative

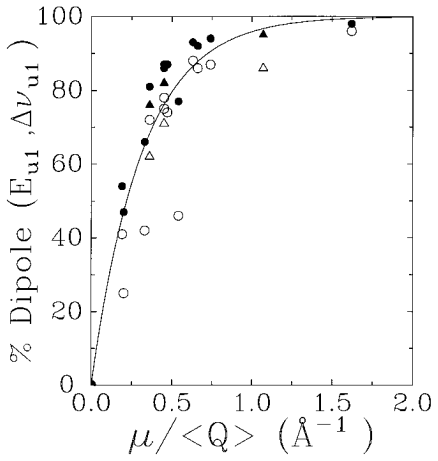

Figure 11. Fraction of the solute−solvent interaction energies contributed by solvent dipole interactions plotted as a function of the dipole/quadrupole ratio of the solvent. Open symbols denote electrostatic interactions with the solute ground-state charge distribution (E_{el}), and filled symbols denote interactions with the difference charge distribution ($\Delta\nu$). The curve through the data is the function % Dipole $= 100[1 - \exp[-3.2(\mu/\langle Q\rangle)]]$.

magnitudes of the individual terms listed, just their absolute magnitudes. Thus, the results in Table 3 are useful guides to the relative importance of different types of interactions responsible for solvation.

The multipole decompositions in Table 3 show several interesting features. First, for solvents with substantial dipole moments (μ > 2D), dipole−solute interactions often dominate in the solvation, accounting for more than 80% of the total interaction in many cases. However, for solvents like benzonitrile and the difluorobenzenes (which also have significant quadrupole and octapole moments), interaction with higher-order moments can be of comparable or even greater importance than the dipolar interactions, despite the large dipole moments these molecules possess. Rather than the size of the dipole moment itself, it is the ratio of the dipole to the quadrupole moments that determines the relative importance of dipolar versus quadrupolar interactions in these solvents. This fact is illustrated in Figure 11, where the dependence of the dipolar contributions E_{u1} and $\Delta\nu_{u1}$ is plotted as a function of the ratio $\mu/\langle Q\rangle$. Although the results for E_{u1} and $\Delta\nu_{u1}$ are similar, the fraction of the solute−solvent interaction contributed by solvent dipole interactions is uniformly larger for the Δq distribution ($\Delta\nu_{ul}$, solid symbols). This is because the difference (Δq) distribution is predominantly dipolar in character whereas that of the ground state is more complex. (For example, the ratio of $\mu/\langle Q\rangle$ for the two coumarin charge distributions is 0.31 and 2.8, respectively.) Thus, the electrostatic potential created by the solute Δq distribution is of longer range and can couple more effectively with the solvent's dipole moment. This difference points out the fact that the decompositions performed here are specific to C153. For other solutes having different shapes and charge distributions, one expects the results to vary somewhat. However, the present results should be representative of the types of solutes used in spectroscopic studies of solvation. The data in Figure 11 can therefore be used as a semiquantitative guide to the relative importance of dipole versus quadrupole interactions in different solvents if the magnitudes of μ and $\langle Q\rangle$ are known.

A general observation that can be made from the data in Table 3 is that, as far as solvation is concerned, most solvents can be categorized as interacting predominantly via one particular charge moment. This is not true of methyl acetate and the dipolar benzene solvents mentioned above, which have important contributions (>20%) from several multipole orders. But for the remaining solvents, especially the nondipolar solvents, the situation is much simpler. Of the nondipolar solvents examined here, all those that possess a significant quadrupole moment derive more than 80% their solvation energetics from quadrupolar ($j = 2$) interactions alone. The remainder comes from smaller hexadecapole ($j = 4$) contributions. (In part, this clean separation comes from the fact that the $j = 3$ terms are zero as a result of the inversion symmetry possessed by the benzenes and most other nondipolar but quadrupolar molecules.) For the solvents that lack both a dipole and a quadrupole moment, the octapolar term completely dominates the interactions. Thus, the present results suggest that it should be possible to gain a reasonable understanding of solvation in many typical solvents using pure point multipole representations: point dipoles, as has long been assumed for dipolar solvents, and point quadrupoles or point octapoles for nondipolar solvents.

VI. Dynamics of Nondipolar Solvation

Although our main emphasis in this paper is on solvation energetics, it is also interesting to briefly consider the dynamics of solvation in nondipolar solvents. We have just shown that the *magnitudes* of the Stokes shifts of C153 can be understood from a single electrostatic perspective, irrespective of whether the solvent is dipolar or whether its nuclear polarizability reflects some higher-order property. The only real difference between the two classes of solvents is that whereas continuum dielectric predictions (i.e., $F(\epsilon_0,n)$) form a good starting point for understanding the energetics in dipolar solvents, in nondipolar solvents they do not. Much the same can be said of the dynamics of solvation. In previous work, we have shown that the time-dependent relaxation of the solvation energy of C153 in dipolar solvents can be accurately modeled based on a knowledge of the frequency-dependent dielectric response of the solvent, $\epsilon(\omega)$.[5] Since $\epsilon(\omega)$ is analogous to $F(\epsilon_0,n)$ in being an infinite-wavelength property, it too fails to convey usable information in the case of nondipolar solvents. However, just as in the case of the energetics, we expect the dynamics of solvation in nondipolar solvents to involve similar reorientational/translational solvent motions as in dipolar solvents, even if they are less readily modeled.

To see whether this expectation is borne out, we have measured the solvation dynamics of C153 in five representative nondipolar solvents, 1,4-dioxane and four aromatic solvents. The results are summarized in Table 4 and in Figures 12−14. Representative time-resolved emission spectra are shown in Figure 12. The dashed curves in each panel represent the steady-state (lowest-frequency curve) and estimated "time-zero" emission spectra that are used to determine the Stokes shift from steady-state data. The spectra shown here are typical of what we observe in nondipolar solvents. Except for the magnitudes of the shifts, they are in no way different from spectra recorded in dipolar solvents. We note that the estimated time-zero spectrum is broader than the observed spectrum at time zero (solid points at high ν) by several hundred wavenumbers. This is also true in dipolar solvents, and it is the major source of uncertainty in the estimation of the Stokes shift magnitudes. Nevertheless, as shown in ref 5, in virtually all cases studied, both the peak and average frequency shifts appear to be accurately reproduced by these estimated time-zero spectra. (See also Table 4.)

The time-resolved spectra are used to determine the spectral response function

TABLE 4: Summary of Solvation Dynamics Results

			Stokes shift[b]		multiexponential fit parameters[c]						characteristic times[d]		
solvent	no.	N^a	$\Delta\nu$ (obs)	$\Delta\nu$ (calc)	a_1	τ_1	a_2	τ_2	a_3	τ_3	τ_0	t_{1e}	$\langle\tau\rangle$
tetrahydrofuran	13	2	1.32	1.30	0.447	0.228	0.553	1.52	0.000	1.00	0.43	0.70	0.94
1,4-dioxane	31	2	1.26	1.25	0.456	0.177	0.520	2.21	0.024	18.30	0.35	0.92	1.67
benzene	35	3	0.83	0.71	0.366	0.234	0.600	1.89	0.034	24.72	0.53	1.12	2.06
hexafluorobenzene	36	2	0.95	0.80	0.292	0.154	0.132	0.71	0.576	6.25	0.46	2.85	3.74
toluene	38	3	0.93	0.64	0.386	0.157	0.512	2.16	0.102	15.21	0.37	1.35	2.72
butylbenzene	39	2	0.67	0.63	0.443	0.192	0.346	5.77	0.211	32.02	0.42	3.77	8.84

[a] Number of independent data sets (spectral reconstructions) used to determine $S_\nu(t)$. [b] Observed and calculated magnitudes (10^3 cm^{-1}) of the time-dependent Stokes shift. For tetrahydrofuran and dioxane (the solvents giving the largest shift) these two shifts were sufficiently close that we used the calculated time-zero spectra to determine the value of $\nu(0)$ to be used in constructing $S_\nu(t)$ (eq 8). For the remaining solvents the values observed in the time-dependent spectra $\nu(0)$ were used directly. [c] Parameters of the multiexponential fit (eq 9) of $S_\nu(t)$. The results shown here correspond to $S_\nu(t)$ data combining the time dependence of both the peak and average frequencies of the time-evolving spectra. (See ref 5 for details.) All times are in picoseconds. [d] Characteristic times, the initial, 1/e, and average time constants (picoseconds) of $S_\nu(t)$ defined in the text.

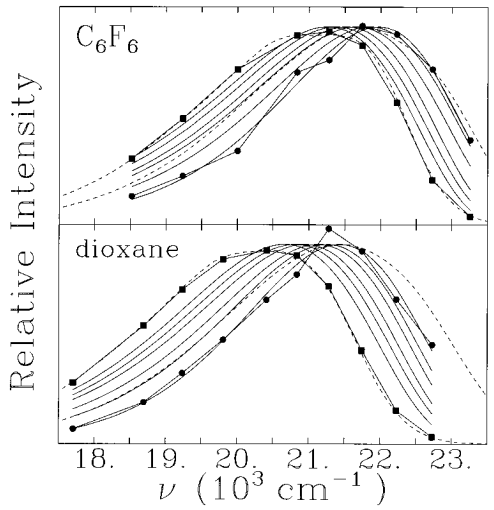

Figure 12. Time-resolved emission spectra of C153 in hexafluorobenzene and 1,4-dioxane. The filled symbols are the reconstructed spectra at times $t = 0$ (circles) and at "long" times (squares). The smooth solid curves are log-normal fits to the reconstructed spectra at intermediate times. The dashed curves in each panel show the estimated "time-zero" and steady-state emission spectra (lower-frequency curve). The spectra shown here correspond to times of 0, 0.1, 0.5, 2, 5, 10, and 50 ps in the top panel and 0, 0.1, 0.2, 0.5, 1, 2, and 20 ps (right to left) in the bottom panel.

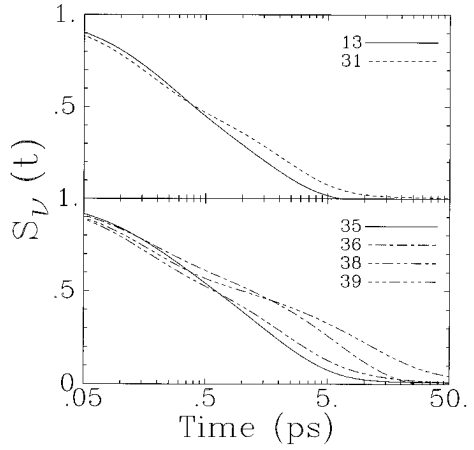

Figure 13. Spectral response functions ($S_\nu(t)$, eq 8) observed in tetrahydrofuran (no. 13) and in the nondipolar solvents: no. 31 = 1,4-dioxane, no. 35 = benzene, no. 36 = hexafluorobenzene, no. 38 = toluene, and no. 39 = *n*-butylbenzene.

based on the behavior of the peak and first-moment frequencies, $\nu(t)$. (Details of the procedures used are provided in ref 5.) In the case of C153, we have shown that this spectral response

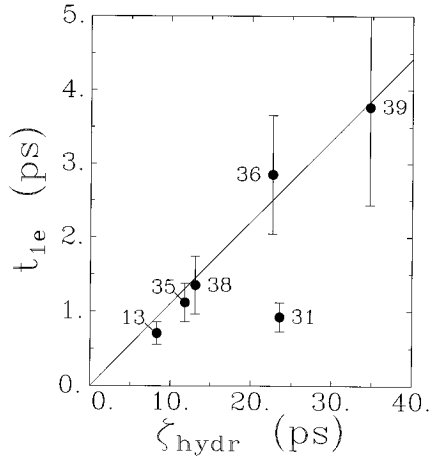

Figure 14. Comparison of the 1/e times of the spectral (or solvation) response functions of Figure 12 with an estimate of the "hydrodynamic friction" ζ_{hydr} operating on the solvent molecules (eq 10). The solvents shown here are no. 13 = tetrahydrofuran, no. 31 = 1,4-dioxane, no. 35 = benzene, no. 36 = hexafluorobenzene, no. 38 = toluene, and no. 39 = *n*-butylbenzene.

$$S_\nu(t) \equiv \frac{\nu(t) - \nu(\infty)}{\nu(0) - \nu(\infty)} \tag{8}$$

function accurately monitors the time dependence of the solvation process.[5]

The $S_\nu(t)$ functions so obtained are plotted in Figure 13. Parametrizations of these response functions in terms of the multiexponential representation

$$S_\nu(t) = \sum_{i=1}^{3} a_i \exp(-t/\tau_i) \quad \text{with} \quad a_i \geq 0 \quad \text{and} \quad \sum_i a_i = 1 \tag{9}$$

are provided in Table 4. Also listed in this table are three characteristic times of $S_\nu(t)$: the initial time constants,

$$\tau_0^{-1} \equiv \sum_i a_i \tau_i^{-1} \tag{10}$$

the 1/e times, t_{1e}, and the average time constants,

$$\langle\tau\rangle \equiv \sum_i a_i \tau_i \tag{11}$$

Whereas t_{1e} is a measure of the overall decay time of $S_\nu(t)$, τ_0 and $\langle\tau\rangle$ respectively emphasize the short- and long-time behavior of the response function.

For comparison, in both Figure 13 and Table 4 we have also included results for one (weakly) dipolar solvent, tetrahydrofuran (THF). As highlighted in the top panel of Figure 13, the dynamics displayed by the nondipolar solvent dioxane are similar to those measured in THF. Given the similarity of the polar groups in the two molecules, and their comparable solvation "mechanisms" as discussed in section III, this similarity is not surprising. Indeed, as anticipated above, the dynamics observed in all of the nondipolar solvents studied here are in no way qualitatively different from the solvation dynamics previously studied in dipolar solvents.[3,5] The dynamics is bimodal in character, consisting of a fast portion associated with inertial solvent motions and a much slower component associated with diffusive dynamics. As can be seen from Figure 13, the inertial components ($+<0.5$ ps) observed for of all of the nondipolar liquids are comparable, involving times on the order of 200 fs and accounting for some 30−50% of the solvation response. In contrast, the diffusive times differ appreciably among the various solvents studied.

Although no simple theories are available with which to accurately model the solvation dynamics in these nondipolar solvents, the similarities and differences in the inertial and diffusive times displayed in Figure 13 can be easily rationalized. The comparable inertial dynamics in all of these solvents follows from their roughly comparable masses and moments of inertia. Benzene and hexafluorobenzene represent the extremes studied. The relevant ratios in these limiting cases are $(M_1/M_2)^{1/2} = 1.5$ and $(I_1/I_2)^{1/2} = 2.3$, and thus the differences in the inertial dynamics are not expected to be large. Although it is difficult to discern from Figure 13, spectral decomposition of the $S_v(t)$ in the manner described in ref 5 shows that the inertial component of hexafluorobenzene is in fact on the order of a factor of 1.5−1.9 times slower than in the other solvents, which are all fairly similar to one another. The fact that the diffusive part of the dynamics differs more significantly among the different solvents can be understood on the basis of the variable magnitude of the friction on the diffusive motion expected in these solvents. This friction can be roughly estimated from the hydrodynamic relation

$$\zeta_{hydr} \cong V\eta/kT \tag{12}$$

where V is the volume of a solvent molecule and η is the solvent viscosity. Other factors being equal, this friction should govern the long-time dynamics, both rotational and translational, of solvent molecules. Figure 14 shows that the observed 1/e times, which mainly reflect the diffusive portion of the solvation response, are reasonably correlated with this hydrodynamic friction. (The 1/e times are used in preference to the average time $\langle\tau\rangle$ because the uncertainties in the former times are smaller. However, the average times behave similarly.) Within the set of aromatic solvents, t_{1e} appears to be directly proportional to ζ_{hydr}, with the 4-fold differences in the observed solvation times being simply related to a 4-fold difference in the friction in these various solvents. Dioxane does not follow the same correlation as the aromatic solvents, presumably due to a difference in how the individual solvent motions contribute to the solvation in this case. More data are clearly needed before much more can be said on this point. However, the above results indicate that the collective dynamics of solvation in these solvents reflects both the underlying single-particle dynamics of the solvent and the nature of the coupling of these single-particle dynamics to the collective solvation coordinate, just as in the case of polar solvents.[39]

Finally, it is useful to comment on the relationship of the present results to the recent studies of nonpolar solvation by Berg and co-workers.[40,41] These authors examined the time-dependent Stokes shifts of the solute dimethyl-*s*-tetrazine (DMST) in *n*-butylbenzene as a function of temperature between 155 and 250 K. At 298 K the magnitude of the Stokes shift in this system was observed to be 95 cm^{-1}, much less than the 600−700 cm^{-1} observed with C153 in butylbenzene. Extrapolating the dynamics observed with DMST to room temperature, it appears that the time dependence of solvation of DMST also differs greatly from that observed with C153. With C153 we find a 1/e time for relaxation of the solvation energy of ∼4 ps. In DMST the inertial (or "phonon") component is much more pronounced, such that we estimate t_{1e} to be only 0.2 ps in this solvent. These large differences in both the magnitude and time scale of the Stokes shift point to fundamental differences in the solvation process being observed in the two cases. We have demonstrated that the highly dipolar nature of the $S_0 \rightarrow S_1$ transition in C153 leads to a solvation mechanism in which the solute and solvent couple via electrostatic interactions (mainly dipole−quadrupole interactions). DMST, on the other hand, is nondipolar by symmetry in both its S_0 and S_1 states. In this case Berg has shown that the solvation can be reasonably modeled in terms of motions modulating the van der Waals interactions between the solute and solvent molecules.[41] Rather than causing a large dipolar perturbation, the electronic transition DMST is interpreted as causing a slight expansion of the solute. The transition is thereby coupled mainly to viscoelastic modes of the solvent, rather than to its dielectric response. Berg[41] and others[42] have shown that the solvation dynamics in this viscoelastic limit need not be very similar to the "dielectric" solvation dynamics studied extensively with solutes like C153.[43] The large differences between the behavior of C153 and DMST in butylbenzene serve to point out that there is no one universal dynamics associated with solvation. Rather, there is a spectrum of dynamics that mirrors the spectrum of possible interactions between solutes and solvents. Although the same solvent−molecule dynamics underlies all cases, how these are manifest in the solvation response depends strongly upon the particular types of solvent−solute coupling present. The DMST and C153 cases appear to represent two extremes of this spectrum. Further study will undoubtedly uncover other new and different cases.

VII. Summary and Conclusions

In this work we have sought to elucidate of the nature of the time-dependent Stokes shifts observed with the dipolar solute coumarin 153 in nondipolar solvents like benzene. Previous studies have shown that continuum dielectric theories provide reasonable predictions for both the static and dynamic aspects of the shifts of C153 in strongly dipolar solvents. It was therefore surprising to find rather large Stokes shifts (500−1000 cm^{-1}) in nondipolar solvents such as benzene, since the same continuum theories predict no appreciable shift in such solvents. The additional steady-state and time-dependent results presented here show that the Stokes shifts in nondipolar solvents are not qualitatively different from the shifts previously studied in dipolar solvents. In all solvents, the magnitudes of the shifts provide a reliable measure of the energetics of the solvent nuclear reorganization elicited by a dipolar solute perturbation, i.e., by a change such as the $S_0 \rightarrow S_1$ transition of C153. These reorganization energies are in all cases dominated by interactions between the solute difference (Δq) charge distribution and the permanent charge distributions of solvent molecules. The only distinction between strongly dipolar solvents and nondipolar solvents is that in the former case the electrostatics mainly involve solvent dipole−solute dipole interactions, whereas in nondipolar solvents the interactions are with the quadrupole and

higher-order multipole moments of solvent molecules. While the latter interactions are not directly reflected in the solvent's dielectric properties (and thus cannot be modeled by continuum dielectric descriptions), these interactions are by no means negligible compared to dipole−dipole interactions.

The finding that nondipolar solvents like benzene exhibit substantial "polarity" is certainly not a new one. For example, the effects of higher-order multipole moments on the thermodynamic properties of liquids have been studied in some detail by Gubbins and co-workers.[44] Molecular manifestations of higher-order polarities can also be found in the so-called aromatic solvent-induced shifts observed in NMR spectra[45] and in the electronic spectral shifts that have long served as the basis for empirical scales of solvent polarity. Indeed, in section III we compared the spectral shifts observed with C153 to two of the most popular solvatochromic scales of solvent polarity, the π^* and E_T^N scales. We found reasonable correlations between the observed shifts and these polarity measures in both dipolar and nondipolar solvents. However, it is important to note that what is being measured in the case of the Stokes shifts of C153 is simpler than in these other polarity indicators. Because the π^* and E_T^N scales both rely on absorption frequency shifts, the characterization of solvent polarity derived from them incorporates elements of both the nuclear and the electronic polarizabilities of the solvent in unknown proportions. An important advantage of examining Stokes shifts (or roughly speaking the difference between emission and absorption shifts) is that they reflect solely that part of the solvent response that is modulated by nuclear motions. In the case of C153 (but not in all cases) this nuclear response is dominated by interactions between the solute and the permanent charge moments of solvent molecules. Electronic polarizability appears to be of negligible importance. Thus, with the present data one is able to cleanly measure one of these two aspects of solvent polarity in isolation. The part measured is of particular interest because it is just this "nuclear reorganization energy" that determines solvent contributions to free energy barriers in electron transfer processes. More importantly, isolation of the nuclear response from the electronic polarizability enables us to provide a particularly simple understanding of differences observed with different solvents.

By using *ab initio* calculations to characterize the permanent charge distributions of a variety of solvent moleucles, we have been able to rationalize the magnitudes of the Stokes shifts observed in all of the solvents studied. In the case of nondipolar but strongly quadrupolar solvents such as benzene, the observed shifts are found to correlate with the magnitudes of the solvent's quadrupole moment. However, in order to understand the Stokes shifts observed in all solvents on an equal footing, one needs to go beyond point multipole approximations and consider the full charge distribution of the solvent. By adopting such a "complete" representation of the interactions between the solute and solvent molecules, we have shown how a crude binary-interaction model for the liquid can be used to correlate the Stokes shifts observed to the strength of solute−solvent interactions *in all solvents*. While this type of modeling is far from realistic as regards solvation structure, it nevertheless demonstrates that the observed shifts are connected in a simple way to interactions between the predominantly dipolar $S_0 \rightarrow S_1$ transition of C153 and the permanent charge distributions of solvent molecules. It would of course be desirable to confirm this connection further through more accurate modeling of the intermolecular correlations present in the real solvents. Raineri and co-workers[46] have very recently formulated a theory of solvation and dielectric response in nondipolar solvents based on integral equation treatments of site−site interactions. Application of their theory to the present systems appears to provide just such a confirmation.[47]

While most of our attention has been focused on the *magnitudes* of the Stokes shifts observed in nondipolar liquids, the time dependence of these shifts, which reflects the dynamics of solvation in such solvents, is also of interest. At least within the series of benzene-like solvents studied here, the variations in the dynamics observed with different nondipolar solvents appear to be simply related to differences in the underlying rotational and translational dynamics of solvent molecules. The "mechanisms" of solvation appear to be comparable to those present in strongly dipolar solvents. However, arriving at a quantitative understanding of solvation dynamics in nondipolar solvents poses a new challenge to theory. Unlike the case of dipolar solvents, where one can use $\epsilon(\omega)$ as a ready source of information on the collective dynamics of the solvent, such an easy starting point is unavailable in the case of nondipolar solvents. In order to extract the relevant friction kernal or memory function for such solvents, one must begin with information that is farther removed from the solvation dynamics of interest. One might, for example, use results of dynamical Kerr effect measurements[48] or information on solvent single-particle autocorrelation functions[39,49] to derive the necessary dynamical information. In either case, however, the connection to the solvation dynamics of interest is considerably less direct. Accurately predicting the dynamics of solvation observed in these systems therefore provides a more stringent test of our understanding of solvation dynamics and its relationship to these other manifestations of solvent-molecule motions than does the case of strongly dipolar liquids, especially since the latter are already reasonably well understood in terms of continuum dielectric models. Hopefully, the experimental results presented here will stimulate further theoretical work along these lines.

Acknowledgment. The authors thank Jennifer Lewis for providing spectra in supercritical solvents, Douglas Fox of Gaussian, Inc., for useful communications about Gaussian 94 and its treatment of quadrupole moments, and Marshall Newton and Fernando Raineri for helpful discussions concerning the nature of nondipolar solvation. This work was supported by funds from the Division of Basic Energy Sciences of the U.S. Department of Energy and made possible by an equipment grant from the Office of Naval Research.

Appendix

The electrostatic interaction energy of two molecules with atom-centered point charges is given by

$$u = \sum_i \sum_j \frac{q_i q_j}{r_{ij}}$$

where the ith point charge on one molecule is a distance r_{ij} from the jth point charge on the other. This energy can be decomposed into contributions from interacting point multipoles. Using the notation of Gray and Gubbins,[19] the interaction energy between a point multipole of order l_1 on molecule 1 and a point multipole of order l_2 on molecule 2 is given by the following expression:

$$u_{l_1 l_2} = \frac{(-1)^{l_1}}{(2l_1 - 1)!!\,(2l_2 - 1)!!} \vec{\vec{\mathbf{Q}}}^{(l_1)} \cdot \vec{\vec{\mathbf{T}}}^{(l_2+l_2)}(\vec{\mathbf{r}}) \cdot \vec{\vec{\mathbf{Q}}}^{(l_2)}$$

Here the Cartesian point multipoles $\mathbf{Q}^{(l)}$ are defined in the symmetric traceless form

$$\vec{\vec{\mathbf{Q}}}^{(l)} = \frac{(-1)^l}{l!}\sum_i q_i r^{2l+1}\vec{\vec{\mathbf{T}}}^{(l)}(\vec{\mathbf{r}})$$

and the gradient tensor is given by

$$\vec{\vec{\mathbf{T}}}^{(l)}(\vec{\mathbf{r}}) = \vec{\nabla}^{(l)}\left(\frac{1}{r}\right)$$

In this multipole expansion of the electrostatic energy, the center dot indicates a full contraction of tensors and $(2l-1)!! = (2l-1)(2l-3)...(5)(3)(1)$. Using these formulas and expressions for the gradient tensor given by Buckingham,[50] we have derived and numerically tested the following expressions for interactions through fourth order in the gradient tensor.

$$u_{01} = [-q_1(\vec{\mathbf{u}}_2\cdot\vec{\mathbf{r}}_{12})]/{r_{12}}^3$$

$$u_{02} = [+q_1(\vec{\mathbf{r}}_{12}\cdot\vec{\vec{\mathbf{Q}}}_2\cdot\vec{\mathbf{r}}_{12})]/{r_{12}}^5$$

$$u_{03} = [-q_1(\vec{\mathbf{r}}_{12}\cdot\vec{\vec{\mathbf{\Omega}}}_2:\vec{\mathbf{r}}_{12}\vec{\mathbf{r}}_{12})]/{r_{12}}^7$$

$$u_{04} = [+q_1(\vec{\mathbf{r}}_{12}\vec{\mathbf{r}}_{12}:\vec{\vec{\mathbf{\Phi}}}_2:\vec{\mathbf{r}}_{12}\vec{\mathbf{r}}_{12})]/{r_{12}}^9$$

$$u_{11} = [-3(\vec{\mu}_1\cdot\vec{\mathbf{r}}_{12})(\vec{\mu}_2\cdot\vec{\mathbf{r}}_{12}) + {r_{12}}^2(\vec{\mu}_1\cdot\vec{\mu}_2)]/{r_{12}}^5$$

$$u_{12} = [+5(\vec{\mu}_1\cdot\vec{\mathbf{r}}_{12})(\vec{\mathbf{r}}_{12}\cdot\vec{\vec{\mathbf{Q}}}_2\cdot\vec{\mathbf{r}}_{12}) - 2{r_{12}}^2(\vec{\mu}_1\cdot\vec{\vec{\mathbf{Q}}}_2\cdot\vec{\mathbf{r}}_{12})]/{r_{12}}^7$$

$$u_{21} = [-5(\vec{\mu}_2\cdot\vec{\mathbf{r}}_{12})(\vec{\mathbf{r}}_{12}\cdot\vec{\vec{\mathbf{Q}}}_1\cdot\vec{\mathbf{r}}_{12}) + 2{r_{12}}^2(\vec{\mu}_2\cdot\vec{\vec{\mathbf{Q}}}_1\cdot\vec{\mathbf{r}}_{12})]/{r_{12}}^7$$

$$u_{22} = {}^1/_3[35(\vec{\mathbf{r}}_{12}\cdot\vec{\vec{\mathbf{Q}}}_1\cdot\vec{\mathbf{r}}_{12})(\vec{\mathbf{r}}_{12}\cdot\vec{\vec{\mathbf{Q}}}_2\cdot\vec{\mathbf{r}}_{12}) - 20{r_{12}}^2(\vec{\mathbf{r}}_{12}\cdot\vec{\vec{\mathbf{Q}}}_1\cdot\vec{\vec{\mathbf{Q}}}_2\cdot\vec{\mathbf{r}}_{12}) + 2{r_{12}}^4(\vec{\vec{\mathbf{Q}}}_1:\vec{\vec{\mathbf{Q}}}_2)]/{r_{12}}^9$$

$$u_{13} = [-7(\vec{\mu}_1\cdot\vec{\mathbf{r}}_{12})(\vec{\mathbf{r}}_{12}\cdot\vec{\vec{\mathbf{\Omega}}}_2:\vec{\mathbf{r}}_{12}\vec{\mathbf{r}}_{12}) + 3{r_{12}}^2(\vec{\mu}_1\cdot\vec{\vec{\mathbf{\Omega}}}_2:\vec{\mathbf{r}}_{12}\vec{\mathbf{r}}_{12})]/{r_{12}}^9$$

$$u_{31} = [-7(\vec{\mu}_2\cdot\vec{\mathbf{r}}_{12})(\vec{\mathbf{r}}_{12}\cdot\vec{\vec{\mathbf{\Omega}}}_1:\vec{\mathbf{r}}_{12}\vec{\mathbf{r}}_{12}) + 3{r_{12}}^2(\vec{\mu}_2\cdot\vec{\vec{\mathbf{\Omega}}}_1:\vec{\mathbf{r}}_{12}\vec{\mathbf{r}}_{12})]/{r_{12}}^9$$

In the above equations, $\mathbf{r}_{12}$ is the vector from the center of mass of molecule 1 to the center of mass of molecule 2; $\vec{\mu}_1$, $\mathbf{Q}_2$, etc., are the dipole on molecule 1 and quadrupole on molecule 2, respectively, and the prefactor $1/4\pi\epsilon_0$ must be included to work in the SI system of units. These results are similar to those derived earlier by Kielich[51] and Rein.[52] However, we differ in sign for the u_{01}, u_{03}, u_{12}, and u_{21} terms and in the coefficients for Rein's u_{22}.

Buckingham,[50] Rein,[52] and others have shown that this formalism is easily extended to treat molecular electrostatic interactions using atom-centered point multipoles which give better convergence. In this work, we have treated the solute coumarin 153 as a collection of atom-centered monopoles interacting with molecule-centered multipoles of the solvent. So, for example, the electrostatic energy of C153 interacting with a solvent dipole is

$$E_{ul} = -\sum_s q_s(\vec{\boldsymbol{\mu}}_2\cdot\vec{\mathbf{r}}_{s2})/{r_{s2}}^3$$

where the sum is over the *s* atomic sites on C153 and $\mathbf{r}_{s2}$ is the vector from the *s*th site to the center of mass on the solvent molecule where the point dipole $\boldsymbol{\mu}_2$ is located.

References and Notes

(1) Ooshika, Y. *J. Phys. Soc. Jpn.* **1954**, *9*, 594. Lippert, E. *Z. Electrochem.* **1957**, *61*, 962. McRae, E. G. *J. Phys. Chem.* **1957**, *61*, 562.

(2) For reviews see: Koutek, B. *Collect. Czech. Chem. Commun.* **1978**, *43*, 2368. Amos, A. T.; Burrows, B. L. *Adv. Quantum Chem.* **1973**, *7*, 289. Mataga, N.; Kubota, T. In *Molecular Interactions & Electronic Spectra*; Mercel Dekker: New York, 1970; Vol. 371. Bakhshiev, N. G.; Knyazhanskii, M. I.; Minkin, V. I.; Osipov, O. A.; Saidov, G. V. *Russ. Chem. Rev.* **1969**, *38*, 740.

(3) For reviews see: Maroncelli, M. *J. Mol. Liq.* **1993**, *57*, 1. Jarzeba, W.; Walker, G. C.; Johnson, A. E.; Barbara, P. F. *Chem. Phys.* **1991**, *152*, 57. Barbara, P. F.; Jarzeba, W. *Adv. Photochem.* **1990**, *15*, 1. For more up-to-date references to recent papers in this field, see refs 4 and 5.

(4) Kumar, P. V.; Maroncelli, M. *J. Chem. Phys.* **1995**, *103*, 3038.

(5) Horng, M. L.; Gardecki, J. A.; Papazyan, A.; Maroncelli, M. *J. Phys. Chem.* **1995**, *99*, 17311.

(6) Fee, R. S.; Maroncelli, M. *Chem. Phys.* **1994**, *183*, 235.

(7) In ref 5 (Figure 10) we showed that the magnitude of the dynamic Stokes shift (as estimated from steady-state spectra; $\Delta\nu$ in Table 1) is highly correlated to the broadening of the spectrum as measured by the inhomogeneous width parameter Γ_{inh} (Table 1). For all solvents studied here we find that $\Delta\nu = c\sigma^2/kT$, where kT is Boltzmann's constant times the temperature and $\sigma = \Gamma_{inh}/\sqrt{8\ln 2}$ and with the constant $c = 1.20 \pm 0.03$ (95%, $N = 46$). The correlation coefficient of the fit is 0.99. This excellent correlation, and the fact that the coefficient is close to the linear response expectation ($c = 1$), provides considerable confidence that the Stokes shifts we determine using time-zero analysis are accurate to the ± 100 cm^{-1} level.

(8) See, for example, the reviews: Bolton, J. R.; Archer, M. D. *Adv. Chem.* **1991**, *228*, 7. Marcus, R. A.; Sutin, N. *Biochim. Biophys. Acta* **1985**, *811*, 265.

(9) Laurence, C.; Nicolet, P.; Dalati, M. T.; Abboud, J.-L. M.; Notario, R. *J. Phys. Chem.* **1994**, *98*, 5807. Kamlet, M. J.; Abboud, J.-L. M.; Abraham, M. H.; Taft, R. W. *J. Org. Chem.* **1983**, *48*, 2877.

(10) Reichardt, C. *Chem. Rev.* **1994**, *94*, 2319.

(11) As estimated from the Claussius−Mossotti equation (see, for example: Bottcher, C. J. F. *Theory of Electric Polarization*; Elsevier: Amsterdam, 1973).

(12) Ma, J.; Bout, D. V.; Berg, M. *J. Chem. Phys.* **1995**, *103*, 9146.

(13) Kamlet, M. J.; Abboud, J. L. M.; Taft, W. R. *Prog. Phys. Org. Chem.* **1981**, *13*, 485.

(14) Marcus, R. A. *J. Chem. Phys.* **1965**, *43*, 1261.

(15) Gaussian 94, Revision B.1: Frisch, M. J.; Trucks, G. W.; Schlegel, H. B.; Gill, P. M. W.; Johnson, B. G.; Robb, M. A.; Cheeseman, J. R.; Keith, T.; Petersson, G. A.; Montgomery, J. A.; Raghavachari, K.; Al-Laham, M. A.; Zakrzewski, V. G.; Ortiz, J. V.; Foresman, J. B.; Cioslowski, J.; Stefanov, B. B.; Nanayakkara, A.; Challacombe, M.; Peng, C. Y.; Ayala, P. Y.; Chen, W.; Wong, M. W.; Andres, J. L.; Replogle, E. S.; Gomperts, R.; Martin, R. L.; Fox, D. J.; Binkley, J. S.; Defrees, D. J.; Baker, J.; Stewart, J. P.; Head-Gordon, M.; Gonzalez, C.; Pople, J. A. Gaussian, Inc., Pittsburgh, PA, 1995.

(16) Hehre, W. J.; Radom, L.; Schleyer, P. v. R.; Pople, J. A. *Ab Initio Molecular Orbital Theory*; Wiley: New York, 1986. Cox, S. R.; Williams, D. E. *J. Comput. Chem.* **1981**, *2*, 304. In fact, the slight overestimation of dipole moments is often looked on as an advantage when performing condensed phase simulations. See for example: Cornell, W. D.; Cieplak, P.; Bayly, C. I.; Gould, I. R.; Merz, K. M., Jr.; Ferguson, D. M.; Spellmeyer, D. C.; Fox, T.; Caldwell, J. W.; Kollman, P. A. *J. Am. Chem. Soc.* **1995**, *117*, 5179.

(17) Chang and Castner [Chang, Y. J.; Castner, E. W., Jr. *J. Phys. Chem.* **1996**, *100*, 2684] have recently performed calculations of the dipole and quadrupole moments of three of the solvents studied here using a higher level of theory (6-31G** BYLP-DFT). Their results are all within 10% of the ones presented here.

(18) Extensive reviews of experimental values of quadrupole moment tensors include: Gray, C. G.; Gubbins, K. E. *Theory of Molecular Fluids*; Oxord: New York, 1984; Vol. 1. Flygare, W. H.; Benson, R. C. *Mol. Phys.* **1971**, *20*, 225. Sutter, D. H.; Flygare, W. H. *Top. Curr. Chem.* **1976**, *63*, 89. Specific references are as follows: (a) Flygare, W. H.; Benson, R. C. *Mol. Phys.* **1971**, *20*, 225. (b) Sutter, D. H.; Flygare, W. H. *Top. Curr. Chem.* **1976**, *63*, 89. (c) Oldag, F.; Sutter, D. H. *Z. Naturforsch.* **1992**, *47A*, 527. (d) Ellenbroek, A. W.; Dymanus, A. *Chem. Phys.* **1978**, *35*, 227. (e) Copeland, T. G.; Cole, R. H. *J. Chem. Phys.* **1976**, *64*, 1741. (f) Czieslik, W.; Wiese, J.; Sutter, D. H. *Z. Naturforsch.* **1976**, *31A*, 1210. (g) Craven, I. E.; Hesling, M. R.; Laver, D. R.; Lukins, P. B.; Ritchie, G. L. D.; Vrbancich, J. *J. Phys. Chem.* **1989**, *93*, 627. (h) Davies, G. J.; Chamberlain, J.; Davies, M. *J. Chem. Soc., Faraday Trans. 2* **1973**, *69*, 1223. (i) Battaglia, M. R.; Buckingham, A. D.; Williams, J. H. *Chem. Phys. Lett.* **1981**, *78*, 421. (j) Stolze, W. H.; Stolze, M.; Hübner, D.; Sutter, D. H. *Z. Naturforsch.* **1982**, *37A*, 1165. (k) Vrbancich, J.; Ritchie, G. L. D. *J. Chem. Soc., Faraday Trans. 2* **1980**, *76*, 648. (l) Buckingham, A. D.; Disch, R. L. *Proc. R. Soc. London* **1963**, *A273*, 275. (m) Amos, R. D.; Battaglia, M. R. *Mol. Phys.* **1978**, *36*, 1517. (n) Ritchie, G. L. D.; Vrbancich, J. *J. Chem. Soc., Faraday Trans. 2* **1980**, *76*, 1245.

(19) Gray, C. G.; Gubbins, K. E. *Theory of Molecular Fluids*; Oxford: New York, 1984; Vol. 1.

(20) Communication with Douglas Fox of Gaussian Inc.

(21) Buckingham, A. D. *Adv. Chem. Phys.* **1967**, *12*, 107.

(22) Ritchie, G. L. D.; Vrbancich, J. *J. Chem. Soc., Faraday Trans. 2* **1980**, *76*, 1245.

(23) (a) Singh, U. C.; Kollman, P. A. *J. Comput. Chem.* **1984**, *5*, 129. (b) Besler, B. H.; Merz, K. M., Jr.; Kollman, P. A. *J. Comput. Chem.* **1990**, *11*, 431.

(24) See, for example: Smith, J. W. *Electric Dipole Moments*; Butterworths: London, 1955.

(25) Gubbins, K. E.; Gray, C. G.; Machado, J. R. S. *Mol. Phys.* **1981**, *42*, 817. Gubbins, K. E.; Gray, C. G. *Mol. Phys.* **1981**, *42*, 842.

(26) Moylan, C. R. *J. Phys. Chem.* **1994**, *98*, 13513.

(27) AMPAC 5.0, Semichem Inc., 7128 Summit, Shawnee, KS 66216, 1994.

(28) The semiempirical calculations were all carried out in the geometry optimized for the S_0 state.

(29) Rechthaler, K.; Kohler, G. *Chem. Phys.* **1994**, *189*, 99. McCarthy, P. K.; Blanchard, G. J. *J. Phys. Chem.* **1993**, *97*, 12205.

(30) Baumann, W.; Nagy, Z. *Pure Appl. Chem.* **1993**, *65*, 1729. Baumann, W.; Nagy, Z.; Maiti, A. K.; Reis, H.; Rodrigues, S. V.; Detzer, N. In *Dynamics and Mechanisms of Photoinduced Electron Transfer and Related Phenomena*; Mataga, N., Okada, T., Masuhara, H., Eds.; Elsevier: Amsterdam, 1992; Vol. 211.

(31) This need for scaling of the semiempirical charges is well-known. In their initial study, Besler *et al*.[23b] recommended a scaling factor of 1.42 when determining ESP fit charges from MNDO calculations. Merz [Merz, K. M. *J. Comput. Chem.* **1992**, *13*, 749] later revised this value to 1.35 for molecules containing C, H, O, and N atoms.

(32) Recent studies (ref 29 and calculations in our laboratory) have tended to indicate that AM1-CI calculations might be superior to MNDO-CI calculations for treating molecules like C153. We did find that the ground- and excited-state dipole moments of C153 were better reproduced by AM1-CI calculations without the need for an *ad hoc* scaling. Such calculations gave values of 6.50 and 14.7 for these moments, respectively. However, the ESP fit charges determined from the AM1 calculations showed a much poorer correlation with the *ab initio* charges than did the MNDO results, the regression coefficient being 0.53 in this particular case. Similar observations and rationalizations for this difference in performance were discussed in the original study of Bessler *et al*.[23b] We also found the components of the quadrupole tensor were in relatively poor agreement with the *ab initio* values even though the overall magnitude $\langle Q \rangle = 21.5$ matched rather well. For these reasons, using the MNDO-CI charges with appropriate scaling seems to offer the best choice for the present purposes.

(33) See also: Carter, A. E.; Hynes, J. T. *J. Chem. Phys.* **1991**, *94*, 5961. Maroncelli, M.; Fleming, G. R. *J. Chem. Phys.* **1988**, *89*, 5044.

(34) Haughney, M.; Ferrario, M.; McDonald, I. R. *Mol. Phys.* **1986**, *58*, 849. Edwards, D. M. F.; Madden, P. A.; McDonald, I. R. *Mol. Phys.* **1984**, *51*, 1141.

(35) These values for the Stokes shifts differ from those previously given in Table 2 of ref 4 by a factor of $(1.24/1.42)^2$, which results from a difference in the choice of scale factors in the ESP fit charges. The value of 1.42 originally recommended by Besler *et al*.[23] was used in the previous study, whereas we employ the value of 1.24 determined specifically for C153 in the present work.

(36) It should be noted that direct comparison of the simulation and experimental values provided here is not completely correct. The reason is that the solvent models used in the simulations of ref 4 lack electronic polarizability; i.e., they have refractive index values of $n^2 = 1$. Continuum dielectric estimates such as eq 1 predict that this neglect of electronic polarization should lead to overestimation of $\Delta\nu$ (∼35%). More sophisticated calculations for the C153 solute also indicate the error should be about 30%.[46] Thus, if one corrected the simulations for the missing electronic polarizability of the solvent, rather than being 10−20% too large, the calculated values would be ∼20% too small compared to the experimental values. In either case, the agreement is rather good, lending confidence in the potential models employed.

(37) Molecular dynamics simulations of C153 in methanol and acetonitrile show that, with the exception of strong hydrogen bonds formed between methanol and the carbonyl group of C153, there is little orientational ordering about either the ground- or excited-state solutes. Some appreciation for the magnitude of the deviations from an isotropic distribution involved in these systems can be obtained by considering C153 to be a point dipole within a spherical cavity and using the experimental solvation energies to compute the average alignment with the solute electric field that would be required within the first solvation shell to produce such energies. The root-mean-square average electric field produced by a point dipole of magnitude μ_u at a distance r is $2^{1/2}\,\mu_u/r^3$. The interaction energy (ϵ) between a solvent dipole μ_v and this average field is $\epsilon = \mu_v \cos\theta$, where θ is the angle the dipole makes with the field. Therefore, in order for n solvent molecules at an average distance a from the solute to produce an average interaction energy of $\langle\epsilon\rangle$, the average alignment ($\langle\cos\theta\rangle$) that would be required is

$$\langle\cos\theta\rangle = \frac{a^3\langle\epsilon\rangle}{2^{1/2}n\mu_v\mu_u}$$

The average interaction energy with the excited state (S_1) can be estimated from the Stokes shift ($\Delta\epsilon$) via $\epsilon_{S1} \equiv \{\mu_{S1}^2/(\Delta\mu)^2\}\Delta\epsilon$. Using values appropriate for C153 in acetonitrile ($\Delta\epsilon = 2320$ cm^{-1}, $\Delta\mu_u \sim 8$ D, $\mu_u = \mu_{S1} \sim 15$ D, $a = 5.8$ Å, $\mu_v = 3.9$ D, and $n \sim 30$), one calculates a value of $\langle\cos\theta\rangle = 0.13$. In other words, first solvation shell molecules are arranged such that the average projection of their dipole moment along the solute's field direction is 13% of μ_v. Thus, even for the highly dipolar S_1 state, the deviation from an isotropic orientational distribution is relatively minor. The effect of this small anisotropy on the energy *fluctuations* of interest here is probably negligible.

(38) Jorgensen, W. L. BOSS Version 3.5, Yale University, New Haven, CT, 1994. Lennard-Jones parameters for C153 were those listed in ref 4. Parameters for CO_2 and CS_2 were respectively from: Bottani, E. J.; Bakaev, V.; Steele, W. A. *Chem. Eng. Sci.* **1994**, *49*, 2931. Tildesley, D. J.; Madden, P. A. *Mol. Phys.* **1981**, *42*, 1137.

(39) Maroncelli, M.; Kumar, V. P.; Papazyan, A. *J. Phys. Chem.* **1993**, *97*, 13.

(40) Fourkas, J. T.; Benigno, A.; Berg, M. *J. Chem. Phys.* **1993**, *99*, 8552. Fourkas, J. T.; Berg, M. *J. Chem. Phys.* **1993**, *98*, 7773.

(41) Berg, M. *Chem. Phys. Lett.* **1994**, *228*, 317.

(42) Bagchi, B. *J. Chem. Phys.* **1994**, *100*, 6658.

(43) However, in some cases, such as propylene carbonate studied in ref 12, viscoelastic and dielectric theories can also lead to very similar predictions.

(44) See, for example: Gubbins, K. E.; Twu, C. H. *Chem. Eng. Sci.* **1978**, *33*, 863. Twu, C. H.; Gubbins, K. E. *Chem. Eng. Sci.* **1978**, *33*, 879.

(45) Nikki, K.; Nakagawa, N. *Magn. Reson. Chem.* **1985**, *23*, 432. Nikki, K.; Nakagawa, N. *Bull. Chem. Soc. Jpn.* **1978**, *51*, 3267.

(46) Perng, B.-C.; Newton, M. D.; Raineri, F. O.; Friedman, H. L. *J. Chem. Phys.* **1996**, *104*, 7153, 7177.

(47) Raineri, F. O. Private communications.

(48) See, for example: Castner, E. W.; Chang, Y. J.; Chu, Y. C.; Walrafen, G. E. *J. Chem. Phys.* **1995**, *102*, 653. Roy, S.; Bagchi, B. *J. Chem. Phys.* **1994**, *101*, 4150. Ladanyi, B. M.; Liang, Y. Q. Interaction-Induced Contributions to Polarizability Anisotropy Relaxation in Polar Liquids. *J. Chem. Phys.*, in press.

(49) Raineri, F. O.; Friedman, H. L. J. *Chem. Phys.* **1994**, *101*, 6111.

(50) Buckingham, A. D. In *Intermolecular Interactions: from Diatomics to Biopolymers*; Pullman, B., Ed.; John Wiley & Sons: Chichester, 1978.

(51) Kielich, S. In *Specialist Periodical Reports*; Davies, M., Ed.; The Chemical Society: London, 1972; Vol. 1.

(52) Rein, R. *Adv. Quantum Chem.* **1973**, *7*, 335.

JP953110E